COMPUTATIONAL FLUID DYNAMICS STUDY OF LOST CIRCULATION PHENOMENON IN NATURALLY FRACTURED RESERVOIRS

FAYSAL AHAMMAD

MASTER OF SCIENCE IN PETROLEUM ENGINEERING

DEPARTMENT OF PETROLEUM AND MINERAL RESOURCES ENGINEERING

BANGLADESH UNIVERSITY OF ENGINEERING AND TECHNOLOGY DHAKA, BANGLADESH

MARCH, 2018

COMPUTATIONAL FLUID DYNAMICS STUDY OF LOST CIRCULATION PHENOMENON IN NATURALLY FRACTURED RESERVOIRS

A THESIS BY

FAYSAL AHAMMAD

SUBMITTED TO THE

DEPARTMENT OF PETROLEUM AND MINERAL RESOURCES ENGINEERING

BANGLADESH UNIVERSITY OF ENGINEERING AND TECHNOLOGY

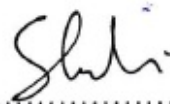IN PARTIAL FULFILLMENT OF THE REQUIREMENTS FOR THE DEGREE OF

MASTER OF SCIENCE IN PETROLEUM ENGINEERING

MARCH, 2018

RECOMMENDATION OF THE BOARD OF EXAMINERS

The undersigned certify that they have read and recommended to the Department of Petroleum & Mineral Resources Engineering, for acceptance, a thesis entitled "**COMPUTATIONAL FLUID DYNAMICS STUDY OF LOST CIRCULATION PHENOMENON IN NATURALLY FRACTURED RESERVOIRS**" submitted by **FAYSAL AHAMMAD** in partial fulfillment of the requirements for the degree of MASTER OF SCIENCE in PETROLEUM ENGINEERING.
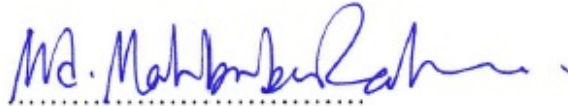
Chairman (Supervisor)

Shahriar Mahmud
Assistant Professor
Department of PMRE, BUET, Dhaka

Member (Ex-Officio)

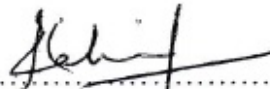Dr. Mohammad Tamim
Professor and Head
Department of PMRE, BUET, Dhaka

Member

Dr. Mohammed MahbuburRahman
Associate Professor
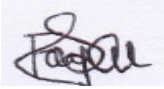Department of PMRE, BUET, Dhaka

Member (External)

Dr. Sheikh Zahidul Islam
Lecturer
School of Engineering
Robert Gordon University
Aberdeen , UK

Date: 7th March, 2018

CANDIDATE'S DECLARATION

I am hereby declaring that no portion of the work considered in this thesis has been submitted elsewhere for the award of any degree or diploma.

………………….

Faysal Ahammad
Student No: 0413132038
Department of Petroleum & Mineral Resources Engineering
BUET, Dhaka

ABSTRACT

Natural Fractures play an important role in oil and gas industry because of their capability of providing pathway for hydrocarbon flow in geologic formations. Fractures connect pores together, therefore, enhance the oil and gas production from a reservoir by increasing the permeability. On the other hand, presence of fractures makes a drilling operation challenging because drilling fluid got lost into them, which in turn increases the drilling cost. The aim of this paper is to carry out a Computational Fluid Dynamics (CFD) study of drilling fluid flow in natural fractures to improve comprehensive understanding of the flow in fractured media.

The study was carried out by creating a three-dimensional steady state CFD model using Ansys (Fluent). For simplicity and validation purpose, the model defines fracture as an empty space between two circular disks. Moreover, it is considered that single phase fluid is flowing through fractures. By solving the flow equations in the model, correlations to determine the fracture width and invasion radius have been developed for specific mud rheological properties. Prior to onset of drilling and at the end of lost circulation, similar correlations can be developed by knowing rheological properties of drilling fluid which will be very much helpful to take an instantaneous action during lost circulation i.e. determining lost circulation material (LCM) particle size and also be useful in the well development stage to determine the damaged area to be treated.

ACKNOWLEDGEMENT

Contents

LIST OF FIGURES

LIST OF TABLES

NOMENCLATURE

v = Drilling fluid velocity inside fracture, ms^{-1}

ΔP = Overbalance pressure, psi

R_i = Invasion Radius, m

Rh = Roughness height, m

k = consistency index, kg/m-s

m = flow behavior index

γc = Critical shear rate, s^{-1}

q = mud loss rate, gallon/minute

R_w = wellbore radius, m

t = time, minute

w = fracture width, m

τ_y = drilling mud yield value, Pa

V = Total mud loss volume, m^3

Chapter One: Introduction

Encountering naturally fractured formations while drilling for oil and gas are very common phenomenon (Reiss, 1980; Van Golf-Racht, 1982; Nelson, 1985). Almost all formations are naturally fractured to some degree. A reservoir fracture system is a complex matrix of inter-connecting and non-connecting fractures (Jones et al., 1988). The area of an individual fracture plane can be varied from a few square inches to several hundred square feet (Parker, 1942; Kelly & Clinton, 1960; Hodgson, 1961). Moreover, a wide range in the spacing of the fractures can be found (Kelly & Clinton, 1960; Parker, 1942). However, fracture spacing of several feet are common (Asfari and Witherspoon, 1973). These fractures are not uniform with parallel walls, but are two dimensional complex networks of variable aperture (Tsang, 1984; Brown and Scholz, 1985; Wang and Narasimhan, 1985; Brown and Kranz, 1986; Schrauf and Evans, 1986; Pyrak Nolte et al., 1988; Morrow et al., 1989). At much lower pressure gradient, viscous and pressure forces become important in fracture flow than in flow through rock matrix. And pressure gradients vary from the wellbore into the formation (Rossen and Kumar, 1992).

Presence of fractures (**Figure 1**) can provide adequate productivity to make a marginally economic reservoir into a commercially productive one. However, while presence of natural fractures is a favorable condition for a reservoir to be highly productive, it can also be a potential source of disaster during drilling operation.
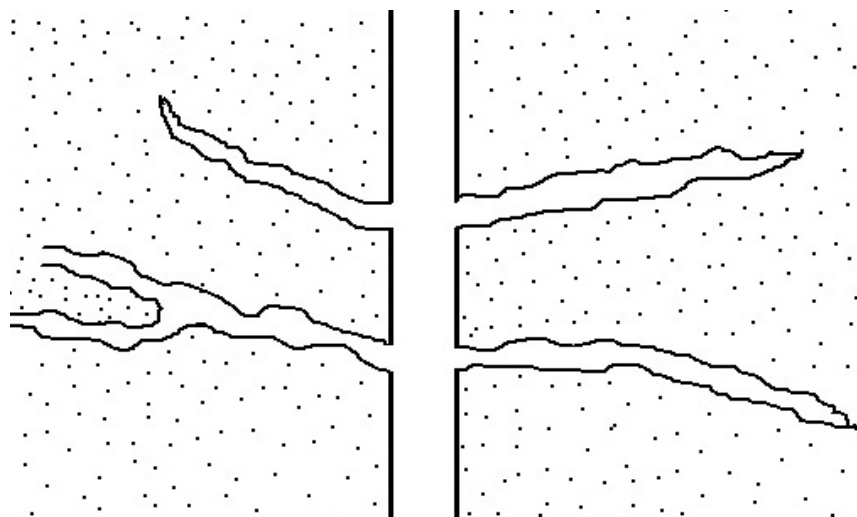
Figure 1.1: Natural Fractures

In particular, fracture can increase the fluid transmitting capability of a reservoir significantly; therefore, any abrupt change in hydrostatic pressure in the wellbore due to the flow of drilling fluid in fractures can give rise to critical well-control issues. If during drilling, a high pressure fractured zone is encountered, formation fluid will flow into the wellbore which may result in a blowout. In contrast, if a low pressure fractured zone is encountered; costly drilling fluid will rapidly flow into the fracture which will reduce the hydrostatic pressure in the wellbore, therefore, posing a risk of sudden flow of formation fluid in the wellbore from the formation above that may ended in a blowout.

During overbalance drilling partial or complete loss of drilling fluid into the fractures is called lost circulation. It is one of the major events that increase Non Productive Time (NPT) in drilling industry. In addition to increasing overall cost of drilling fluid, lost circulation may result in some negative consequences such as stuck pipe, reduced drilling rate, induced kick and the loss of entire well or wellbore (Feng et al. 2016). According to the published data, in Gulf of Mexico 12% of the NPT is caused by lost circulation (Wang et al. 2007), and 10% to 20% of the drilling cost of high-temperature and high-pressure wells is related to lost circulation (Cook et al. 2011). There are various reasons that can cause lost circulation. Complete mud losses occur in heavily fractured formation while partial losses with mud gains occur when a fracture of limited extension is encountered if the pumps are shut down and the circulation is stopped. In non-fractured shale formation, lost circulation has been attributed to the borehole wall deformation (Gill 1989).

As loss of drilling mud i.e. lost circulation is a common event in overbalanced drilling, therefore, it is very important to build a model to know about this phenomenon in detail and with that aim many researchers have tried so far to model this. Modeling drilling fluid flow inside fracture has been a topic of research since the 1990's (e.g., Liétard et al. 1996, Sanfillippo et al. 1997; Maglione et al. 1997; Lavrov and Tronvoll 2004; Majidi et al. 2008; Lavrov 2013 etc.).

Lost circulation is a critical issue that can raise different problems during drilling operation. Moreover, lost fluid will have a negative impact on the productivity of the reservoir because it will reduce the porosity and permeability of the reservoir if not properly treated. Hence, it is very crucial to know about the behavior and flow pattern of the drilling mud inside fracture to facilitate a proper treatment scheme instantaneously. Successful remediation of lost circulation is possible if the underlying physics understood clearly, and for this understanding the mud flow inside fractures is necessary.

Because of the complexity, it is difficult to understand the flow of drilling fluid inside fractures from analytical equations and experiments. Therefore, it is necessary to develop a lost circulation model that would help to better understand the flow of drilling fluid inside fractures. Among all of the Non-Newtonian models, Yield Power Law (YPL) model can more accurately predict the behavior of drilling fluid (Hemphill et al. 1993) because of that YPL model is selected to study the behavior of drilling mud inside fractures. As Computational Fluid Dynamics (CFD) is a useful technique that can help visualize a complex problem more easily; besides, so far no CFD

study has been conducted to understand the behavior of YPL fluid inside fractures; therefore, the purpose of this study is to carry out a CFD study to better comprehend the behavior of drilling fluid inside fractures.

Research Aims and Objectives:

The main focus of this M.Sc thesis is to develop three-dimensional steady state computational models of drilling fluid flowing through a smooth walled and rough walled fracture and find out a way to mitigate drilling fluid loss through fractures using CFD. The aims and objectives of the M.Sc dissertation are summarized as follows:

Aims:

To develop three-dimensional CFD model to better comprehend the flow of drilling fluid inside natural fractures.

Objectives:

(i) Eradicate the need of conventional analytical calculation and type curve matching technique to determine the fracture width.

(ii) Enable driller to mitigate lost circulation instantaneously by selecting proper Lost Circulation Material (LCM)

Chapter Two: Literature Review

Drilling mud is continuously circulated into the wellbore to transport cuttings to the surface, cooling the bit and balance between hydrostatic pressure in the wellbore and formation pressure. The loss of drilling mud is a common scenario while drilling through naturally fractured formations. Apart from that, drilling mud also got lost into the formation through pores and induced fractures. The distinction between different types of fluid loss can be made by observing the mud losses in the mud tank. For natural fractures, there is a rapid initial loss of drilling mud which declines with time; whereas for mud loss through pores, the loss rate increases gradually as the flow of drilling mud increases (Dyke et al. 1995).During overbalance drilling, when a fracture is encountered, drilling mud will flow naturally into the fracture due to existing pressure gradient between the wellbore and the fracture. Till now, many authors have tried to understand the behavior of drilling mud inside fractures characterizing the mud as Newtonian and Non-Newtonian fluid (**Figure 2.1**). The summary of those works given below:
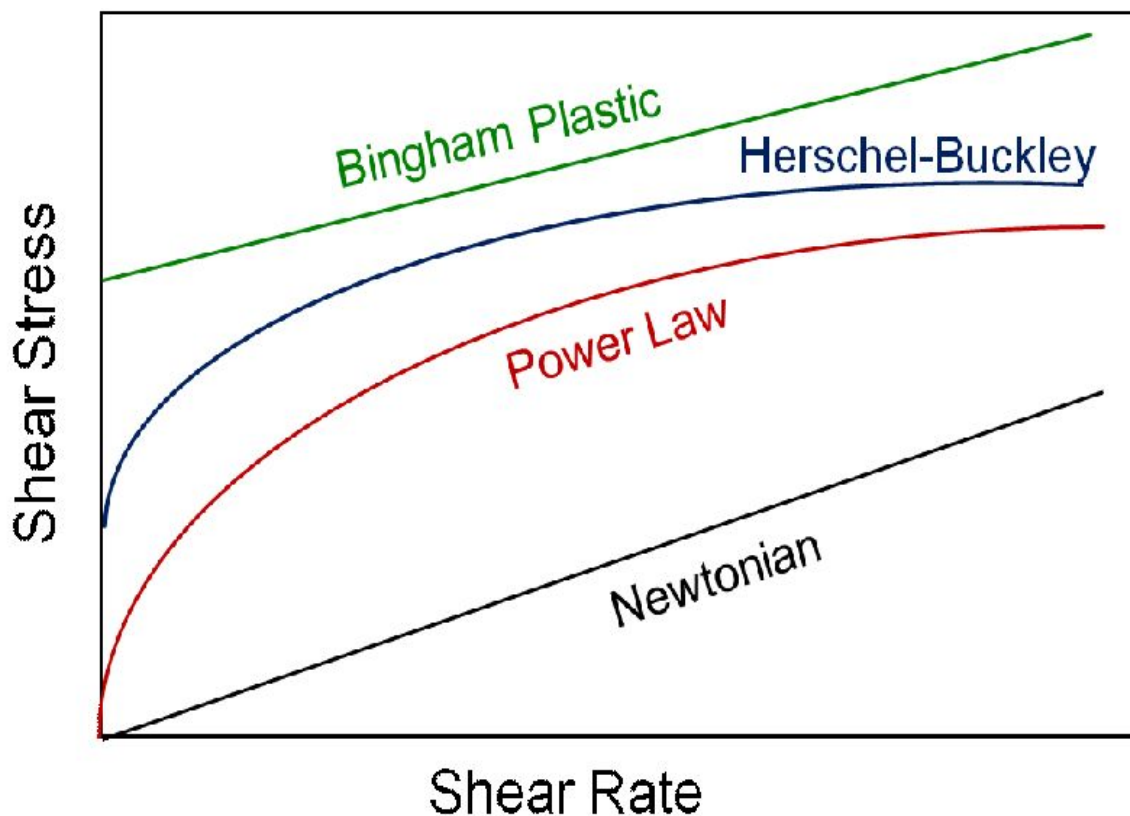
Figure 2.1: Newtonian and Non-Newtonian Rheological Models

Newtonian Fluid:

Newtonian fluid is any fluid that follows Newton's law of viscosity which states that applied stresses is proportional to shear rate i.e.

$$\tau = \mu\gamma \dots \dots \dots \dots \dots \dots \dots (1)$$

Where τ is the shear stress, μ is the viscosity and $\dot\gamma$ is the shear rate

The flow of Newtonian fluid in fractures is well researched. There have been numerous works done on Newtonian fluid flow inside fractures. Initially, fluid flow in fractures was understood using parallel plate model (Huitt, 1955; Snow, 1965). Considering this model, Wtherspoon et al. (1980) developed the classical cubic law equation for steady state isothermal, laminar flow between two smooth walled parallel plates:

$$Q = 5.11 \times 10^6 \left[\frac{W\Delta Pb^3}{L\mu}\right] \dots \dots \dots \dots \dots \dots (2)$$

Where Q= flow rate (bbl/day), W= Width of the fracture face (ft), ΔP= Pressure differential (psi), b= fracture aperture (in), L= length of fracture (ft), μ= fuid viscosity (cp)

Later, Jones et al. (1988) applied Bernoulli's equation for flow in pipes to natural fractures and build an equation for single phase laminar and turbulent flow calculations. The equation is:

$$Q = 5.06 \times 10^4 W[\frac{\Delta Pb^3}{fL\rho}]^{0.5} \dots \dots \dots \dots \dots \dots (3)$$

Where f= friction factor, ρ= fluid density lb/cu ft

Assuming laminar flow of Newtonian fluid flowing radially into highly conductive circular fractures, Sanfillippo et al. (1997) developed a model to estimate width of the fracture and to describe how drilling fluids fill natural fractures during drilling operation. The model is based on radial diffusivity equation:

$$\frac{\partial^2 p}{\partial r^2} + \frac{1}{r}\frac{\partial p}{\partial r} = \frac{\emptyset_{frac}\mu_{mud}C_{mud}}{k_{frac}}\frac{\partial p}{\partial t} \dots \dots \dots \dots \dots \dots (4)$$

Poiseuille's law is valid for this model. Therefore, the fracture width (w) is linked with fracture permeability (k) by the following equation:

$$k = \frac{w^2}{12} \dots \dots \dots \dots \dots \dots (5)$$

Solving radial diffusivity equation assuming constant terminal pressure boundary condition and substituting equation (2) into it yields:

$$a \frac{\dfrac{w^2 t}{12\mu_{mud}\varnothing_{frac}C_{mud}r_w^2}}{\ln\dfrac{w^2 t}{12\mu_{mud}\varnothing_{frac}C_{mud}r_w^2}} - \frac{V(t)}{2\pi\varnothing_{frac}C_{mud}r_w^2 w\Delta P} = 0 \dots\dots\dots\dots\dots (6)$$

Where a is a constant equal to 2.01, ΔP is the overbalance pressure, w is the width of the fracture, t is the time, μ_{mud} is the mud Newtonian viscosity, $\varnothing_{frac}$ is the fracture porosity, C_{mud} is the mud compressibility, r_w is the wellbore radius, and V(t) is the cumulative volume of mud lost in the fracture at time t.

Apart from theoretical works, many authors had carried out experiments (Jones et al., 1988) and simulation to comprehend the flow Newtonian fluid inside fractures (Asfari and Witherspoon, 1973; Douglas et al., 1987; Yang et al., 1989; Sarkar et al., 2002; Cardenas et al., 2007; Koyama et al., 2008)

However, the studies described above are not applicable to common drilling fluids as they are Non-newtonian. The rheological behavior i.e. flow behavior index, consistency index and yield stress of drilling fluid have considerable effect on lost circulation. Moreover, assumption of Newtonian mud leads to an unrealistic invasion radius i.e. infinity.

Bingham Plastic Fluid:

Bingham plastic fluid is defined as the fluid that follows the Bingham plastic model which can be expressed mathematically by the following equation:

$$\tau = \tau_y + \mu_p\gamma \dots\dots\dots\dots\dots\dots (7)$$

Where τ= shear stress, τ_y= yield stress, μ_p= plastic viscosity

Liétard et al. (1996, 1999) developed a model based on Darcy's law to describe the flow of Bingham plastic fluid inside fractures. They assumed the flow regime is laminar and drilling mud is flowing radially into a smooth walled fracture of constant aperture for a constant drilling overbalance pressure. The flow behavior of drilling fluid inside fractures can be known by solving the following equation describing local pressure drop due to laminar flow of bingham plastic fluid in a slot of constant width (w):

$$\frac{dp}{dr} = 12\mu_p \frac{V(r,t)}{w^2} + \frac{3\tau_y}{w} \dots\dots\dots\dots\dots\dots (8)$$

Where p is pressure, μ_p is plastic viscosity τ_y is the yield stress of the drilling fluid, and V(r, t) is fluid velocity for radial flow, equal to:

$$V(r,t) = \frac{1}{2\pi rw}\frac{dV_m}{dt} \dots\dots\dots\dots\dots\dots (9)$$

Then, the amount of mud loss V_m can be evaluated by integrating equation (5):

$$V_m(t) = \pi w[r_i^2(t) - r_w^2] \dots \dots \dots \dots \dots \dots (10)$$

Where r_i is the invasion radius at time t

Substituting equation (5) and (6) into equation (4):

$$\frac{dt_d}{dr_d} = \frac{4r_d \ln r_d}{1 - \alpha(r_d - 1)} \dots \dots \dots \dots \dots \dots (11)$$

Where dimensionless radius, $r_d = \frac{r(t)}{r_w}$; dimensionless time, $t_d = \frac{w^2}{r_w^2}\frac{\Delta P}{3\mu_p}t$ and mud invasion factor, $\alpha = \frac{3r_w}{w}\frac{\tau_y}{\Delta P}$ and ΔP is the constant overbalance pressure.

Several authors worked on Liétard model to solve equation (11) analytically and estimate fracture width without using type curves. Firstly, Sawaryn (2001) found an analytical equation (11):

$$t_d = \frac{4r_{dmax}\ln(r_{dmax})}{\alpha}\left[\{\ln\left(\frac{r_{dmax}-1}{r_{dmax}-r_d}\right) - \frac{r_d-1}{r_{dmax}}\} + \frac{4r_{dmax}}{\alpha}\sum_{n=2}^{\infty}\frac{1}{n}\left(\frac{1}{r_{dmax}}\right)^n\{\ln(r_{dmax}) + \frac{1}{n}\}\right.$$
$$\left. - r_d^n\{\ln\left(\frac{r_{dmax}}{r_d}\right) + \frac{1}{n}\}\right] \dots \dots \dots \dots \dots \dots (12)$$

Later, Civan& Rasmussen (2002) also provided an analytical solution of equation (7):

$$t_d = 4r_{dmax}(r_{dmax}-1)\left[-\ln r_d\{\frac{r_d}{r_{dmax}} + \ln(1 - \frac{r_d}{r_{dmax}})\} + \sum_{n=2}^{\infty}\frac{1}{n^2}\{\left(\frac{1}{r_{dmax}}\right)^n\right.$$
$$\left. - \left(\frac{r_d}{r_{dmax}}\right)^n\}\right] \dots \dots \dots \dots \dots \dots (13)$$

Further improvement was done by Huang et al. (2011) who eradicated the necessity of type curve matching by deriving a cubic equation to determine fracture width (w) using known values of wellbore radius (r_w), overpressure ratio ($\frac{\Delta P}{\tau_y}$), and the maximum mud-loss volume (v_{max}):

$$\text{Fracture width, w} = \left[\frac{\frac{9v_{max}}{\pi}}{\left(\frac{\Delta P}{\tau_y}\right)^2}\right]^{\frac{1}{3}} \dots \dots \dots \dots \dots \dots (14)$$

In contrast to the model proposed by Lietard et al. (1996, 1999) model, Maglione et al. (1997, 2000) studied the flow of Bingham plastic fluid inside fractures based on radial diffusivity

equation. Assuming drilling mud behaves as Bingham Plastic fluid and flowing radially into the fracture of constant width; thus solving the radial diffusivity equation under steady stateconditions the bottomhole drilling overpressure ΔP can be expressed as:

$$\Delta P(t) = \frac{6Q_{loss}\mu_p}{\pi w^3} \ln \frac{\left(\frac{V(t)}{\pi w^2} + r_w^2\right)^{\frac{1}{2}}}{r_w^2} \ldots \ldots \ldots \ldots \ldots \ldots (15)$$

Where Q_{loss} represents mud loss rate as recorded by the flowmeter, r_w is the wellbore radius, μ_p is the plastic viscosity of the drilling mud and $V(t)$ is the cumulative mud loss into the fracture at any time t.

In addition, Amadei& Savage (2001) derived a time dependent solution for Bingham plastic fluid flowing into the fracture with an empirical correction for fracture roughness. Mitsoulis&Huilgol (2004) numerically investigated the flow of Bingham plastic fluid inside fracture with abruptly changing aperture.

More recently, assuming drilling fluid as Bingham plastic, Razavi et al. (2017) developed a model incorporating leak-off phenomenon to describe the flow of drilling mud inside fractures. However, it is not realistic to assume the drilling mud as Bingham plastic fluid as it can't describe the shear thinning and shear thickening of the drilling fluid.

Power Law Fluid:

Power law fluid is the fluid that follows the power law model:

$$\tau = K \left|\frac{\partial V}{\partial Z}\right|^{n-1} \frac{\partial V}{\partial Z} \ldots \ldots \ldots \ldots \ldots \ldots (16)$$

Where n is the flow behavior index; K is the consistency index, $\frac{\partial V}{\partial Z}$ is the shear rate

At n<1 the fluid shear thinning and at n>1 the fluid has the shear thickening behavior. This model is not applicable at low shear rates as viscosity would become infinite at $\frac{\partial V}{\partial Z}$=0. In that situation it is more realistic to consider the fluid as carreau or cross fluid.

Considering the drilling mud as power law fluid, Lavrov (2004, 2014) proposed a model to describe the flow drilling mud inside fractures. In their model, they assume that fracture is already filled with a fluid and defined fracture width as:

$$w = w_0 + \frac{P}{K_n} \ldots \ldots \ldots \ldots \ldots \ldots (17)$$

Where, P is the local fluid pressure inside fracture; K_n is the proportionality co-efficient between fracture width increment and fluid pressure increment and w_0 is the fracture width when the fluid pressure inside the fracture is zero.

Considering stated assumptions, they developed a differential equation of drilling mud flowing into a deformable horizontal fracture of finite length:

$$\frac{\partial w}{\partial t} - \frac{n w^{\frac{2n+1}{n}}}{(2n+1)2^{\frac{n+1}{n}}K^{\frac{1}{n}}} \frac{1}{r} \frac{\partial P}{\partial r}\left(\frac{\partial P}{\partial r}\right)^{\frac{1-n}{n}} - \frac{n}{(2n+1)2^{\frac{n+1}{n}}K^{\frac{1}{n}}} \frac{\partial}{\partial r}\left[w^{\frac{2n+1}{n}} \frac{\partial P}{\partial r}\left(\frac{\partial P}{\partial r}\right)^{\frac{1-n}{n}}\right]$$
$$= 0 \dots \dots \dots \dots \dots \dots (18)$$

Only few experiments on power law fluid have been done so far. Auradou et al. (2008, 2010) carried out experiments assuming the fluid as Carreau fluid and flowing between two parallel rough surfaces. On the other hand, Di Federico (1997) and Lavrov (2013) numerically investigated the Power law fluid flow inside rough fractures and found out that the ratio of the equivalent fracture width to the actual fracture width increases with increasing roughness and flow behavior index.

However, power law model doesn't incorporate yield stress whereas yield stress has considerable effect on total mud loss volume.

Yield Power Law Fluid:

A Yield power law fluid also known as Herschel-Bulkley fluid can be described mathematically as follows:

$$\tau = \tau_0 + k\gamma^n \dots \dots \dots \dots \dots \dots (19)$$

Where τ= shear stress, τ_0= yield stress, k= consistency index, n= flow behavior index and γ= shear rate.

Not much research work has been done on fracture flow of Yield Power Law (YPL) fluid. Majidi et al. (2008) developed a model by characterizing the drilling fluid as YPL fluid to more accurately predict the behavior of drilling fluids inside fracture. Like Liétard et al. (1999), they also provided type curve describing mud loss volume vs. time to determine the fracture width and predict the maximum volume of mud loss based on:

$$\frac{dr_d}{dt_d} = \frac{[1 - \alpha(r_d - 1)]^{\frac{1}{m}}}{2^{\frac{m+1}{m}}r_d\left(\frac{r_d^{1-m}-1}{1-m}\right)^{\frac{1}{m}}} \dots \dots \dots \dots \dots \dots (20)$$

They defined dimensionless radius, $r_d = \frac{r(t)}{r_w}$; dimensionless time, $t_d = \frac{m}{2m+1} \left(\frac{w}{r_w}\right)^{\frac{m+1}{m}} \left(\frac{\Delta P}{K}\right)^{\frac{1}{m}} t$ and dimensionless mud invasion factor, $\alpha = \frac{2m+1}{m+1} \frac{2r_w}{w} \frac{\tau_y}{\Delta P}$

Where m is the flow behavior index; K is the consistency index

Chapter Three: Methodology

Computational Fluid dynamics (CFD) method is used in this study to analyze the flow behavior of drilling fluid inside fractures because CFD makes it possible to numerically solve flow, mass and energy balances in complex geometries like fractures. The details of the flow behavior of YPL type drilling mud inside fractures is identified by numerical simulation using a commercial CFD software, FLUENT, based on structured meshes.

Modeling Domain and Assumptions:

To numerically simulate the flow YPL type drilling fluid flow through fractures, 2m cross section of a wellbore with a radius of 0.11m and a circular shaped smooth walled fracture with a radius of 1m and a width of 880µm are created using the built-in geometry software in FLUENT as shown in **Figure 1.1**. The computational domain is the space between wellbore wall and the drilling pipe as shown in, and the space between two circular disks as shown in **Figure 3.1** and **Figure 3.2**.

The following assumptions were made to develop the CFD model:

- Fracture geometry is empty space between two parallel disk and perpendicular to the wellbore
- Fracture is smooth walled and the fracture walls are impermeable.
- Fluid is single phase YPL type fluid and flow pattern is laminar
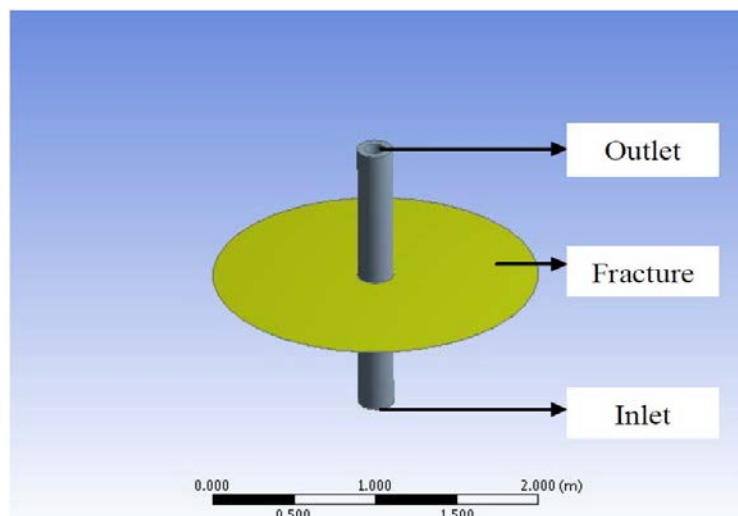
Figure 3.1: Circular fracture perpendicular to the wellbore
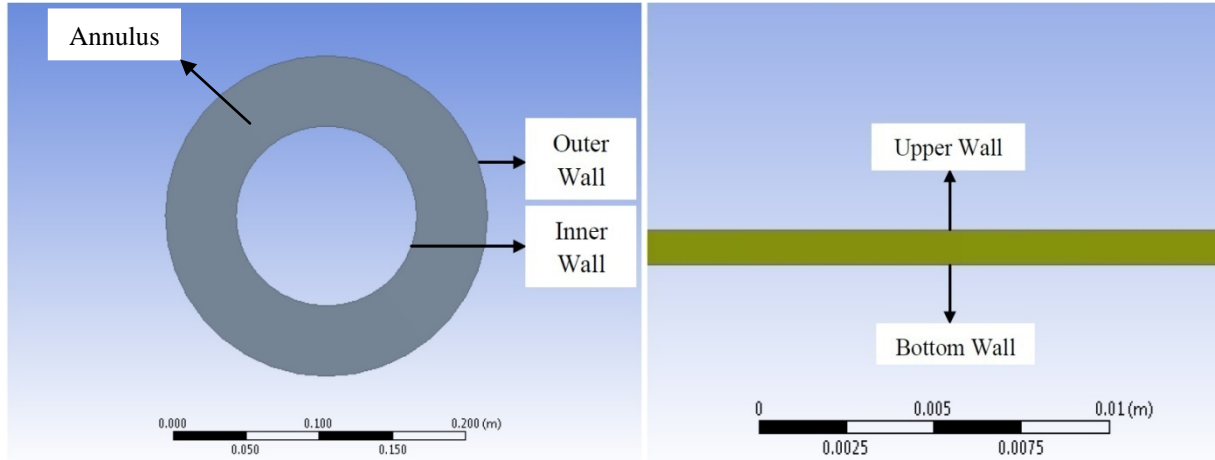
Figure 3.2: Cross section of the wellbore (Left) and Side view of the fracture (Right)

Model Equations:

The governing equations for the steady-state YPL fluid flow model consist of conservation of mass and momentum. The Navier-Stokes equations of conservation of mass and momentum were was used order to model the steady state, incompressible, laminar flow of YPL type of fluid inside fracture. The conservation of mass is given as,

$$\nabla \cdot v = 0 \dots \dots \dots \dots \dots (21)$$

And the conservation of momentum is described by,

$$\rho(v \cdot \nabla)v = -\nabla P + \mu \nabla^2 v \dots \dots \dots \dots \dots (22)$$

Where, v is the velocity vector, ρ is the density, μ is the viscosity and ∇P is the pressure gradient.

Herschel-Bulkley-Papanastasiou Model:

The rheology equation for Herschel-Bulkley (HB) or Yield Power Law fluid is given by equation 19. The presence of yielded and unyielded zone in the flowing drilling mud will create discontinuity in the first order velocity derivative and cause instability in the numerical solution. To avoid this situation, Papanastasiou introduced a material parameter in the HB model that controls the exponential growth of stress. The rheology equation given below is valid for both yielded and unyielded zones:

$$\tau = \tau_0[1 - \exp(-m\gamma)] + k\gamma^n \dots \dots \dots \dots \dots (23)$$

where m is the stress growth exponent

The apparent viscosity is given by:

$$\mu_{apparent} = \frac{\tau_0}{|\gamma|} [1 - \exp(-m|\gamma|)] + k|\gamma|^{n-1} \dots \dots \dots \dots \dots (24)$$

At low shear rates, this equation will produce high viscosity due to the presence of plug flow zone. To overcome this issue and closely imitate the ideal flow behavior of viscoplastic fluid, Papanastasiou suggested that stress growth exponent should be greater than 1000. To calculate apparent viscosity as defined in **Eq. 24**, a user defined function (UDF) written in C attached to FLUENT 17.0 solver. The UDF is shown in **Appendix A.**

Computational Domain and Physical Parameters:

The computational domain consists of a section of wellbore and a penny shaped fracture perpendicular to the wellbore (**Figure 3.1** and **Figure 3.2**). The geometry of fracture and mud properties is similar to the work of Majidi et al. (2008). There is an entrance and an exit region in the computational domain to avoid the effect of inflow and outflow. Symmetrical boundary condition at the inlet and outlet region is considered: constant velocity boundary condition at the inlet and constant pressure boundary condition at the outlet. Physical dimensions of the computational domain and different parameters are given in **Table 3.1**.

Table 3.1: Physical parameters and boundary conditions used for smooth walled fracture simulation

Total wellbore length below and above the fracture, L = 2 m
Wellbore radius, r_w = 0.11 m
Fracture Radius, r = 5 m
Fracture width, w = 880 µm
Overbalance pressure, Δp = 200, 500, 800 and 1000 Psi
consistency index, k = 0.04 kg/m-s
flow behavior index, m = 0.94
Yield stress, τ_y = 4.022 Pascal
critical shear rate, γ_c = 0.01 S^{-1}

The meshes of the computational domain are generated using the built-in meshing software in FLUENT as shown in **Figure 3.3**. As the computational domain is simple, structured grid is adopted. Generally, smaller grid size in the computational domain will produce more accurate results but requires more computation time. Moreover, smaller grid size may cause numerical instability.
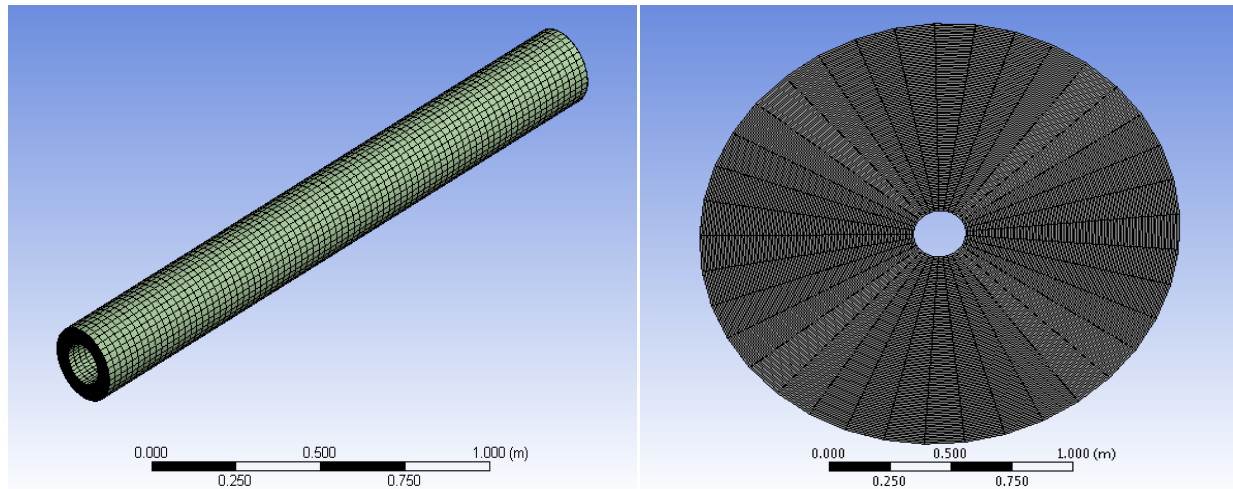
Figure 3.3: Structured mesh of the fracture (Left) and Structured mesh of the wellbore (Right)

Therefore, to select the proper grid size, a sensitivity analysis of the obtained results to the mesh resolution was carried out to ensure the accuracy of the numerical simulations. Using face meshing option and internally dividing different faces it was found out that for total nodes of 388241 and total elements of 377400, the simulation produce more accurate results with less computation time. Based on the results of the analysis, this mesh is used to numerically simulate the YPL type drilling fluid flow through fractures. Simulations have been carried out on a quad core i3 workstation and each simulation took approximately 1000 iterations to converge in approximately 20 minutes of run time.

Table 3.2: Mesh Convergence study (when Δp=200 psi and R_i=1 m)

No. of elements	Fracture Velocity, ms^{-1}	Convergence time, minutes (Approx.)
283000	2.25	10
320700	2.14	15
377400	2.07	20
430890	2.0697	30
489600	2.0694	35

Numerical Procedure:

The governing equations have been solved to investigate the flow of YPL drilling fluid inside a fracture using a finite-volume computational fluid dynamics (CFD) method. The pressure term in the governing equations has been discretized by second-order and the momentum term by the second order upwind scheme. The Semi Implicit Method for Pressure Linked Equations (SIMPLE) algorithm was used for the pressure–velocity coupling. In CFD analysis, SIMPLE algorithm has been widely used to numerically solve the Navier-Stokes equations. To clarify the

procedure, the algorithm is shown is **Fig 3.3**. The solution of the governing equations was considered to be converged when the residual reached below 10^{-6}.

```
                              ┌─────────┐
                              │  Start  │
                              └────┬────┘
   ┌──────────────────┐            │
   │ Herschel-Bulkley │────────────┤
   │    model UDF     │            ▼
   └──────────────────┘   ┌──────────────────┐
                          │  Set boundary and│
                          │ initialization   │
                          │   conditions     │
                          └────────┬─────────┘
                                   ▼
                          ┌──────────────────┐
                          │  Initialization  │
                          └────────┬─────────┘
                                   ▼
                          ┌──────────────────┐
                          │ Solve the        │
                          │ momentum equation│
                          │ to get velocity  │
                          └────────┬─────────┘
                                   ▼
                          ┌──────────────────┐
                          │ Solve the        │
                          │ pressure         │
                          │ correction eq    │
                          └────────┬─────────┘
                                   ▼
                          ┌──────────────────┐
                          │ Correct velocity │
                          │   and pressure   │
                          └────────┬─────────┘
 ┌────────┐                        ▼
 │ Repeat │◄───┐    No      ┌──────────────┐   Yes   ┌─────┐
 └────────┘    └────────────│ Check for    │─────────│ End │
                            │ convergence  │         └─────┘
                            └──────────────┘
```
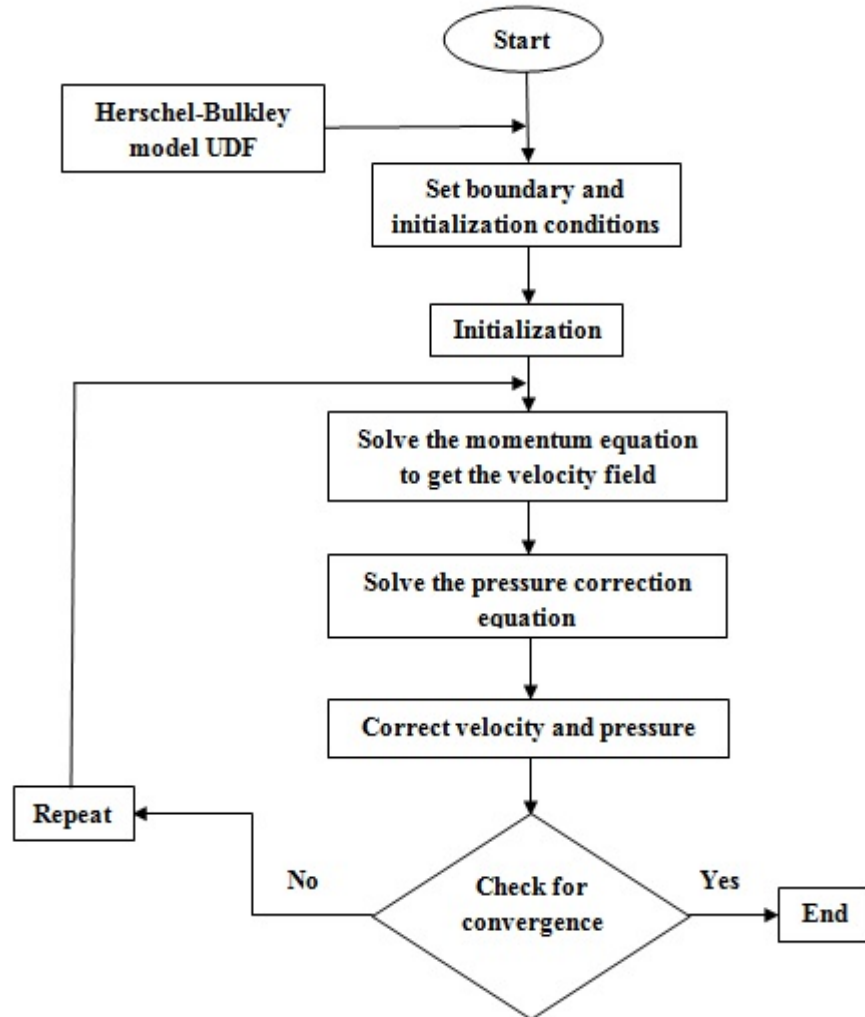
Figure 3.3: Flow chart of SIMPLE algorithm

Chapter Four: CFD Results

Smooth Walled Fracture:

The study was carried out by considering that YPL type drilling fluid is flowing from the bottom of the wellbore through the smooth walled annulus to the smooth walled fracture and there is no loss of fluid through the wall of the fracture as it is considered as impermeable. Values of average velocity of the drilling fluid inside fracture at different fracture radius were obtained by volume integral along the fracture at overbalance pressure of 200 Psi, 500 Psi, 800 Psi and 1000 Psi. Drilling fluid velocity obtained from the simulation then plotted against respective fracture radius. The Cartesian plots in **Figure 4.4** show the relationship between velocity of drilling fluid in fracture and fracture radius for a particular overbalance pressure. These figures show that velocity of YPL fluid inside fractures is less if the overbalance pressure is less. As the overbalance pressure decreases from 1000 psi to 200 Psi the velocity curve shifts toward bottom. As a matter of fact, it means that lesser the overbalance pressure the lesser will be the loss of drilling fluid inside fractures. Furthermore, it can be seen from the figure that the velocity of the drilling fluid decreases rapidly within 2m of the fracture and ahead of that region velocity decreases slowly. This occurs due to the sudden disturbance in the flow and because of that disturbance frictional pressure loss is higher in that region (**Figure 4.1**) due to which velocity decreases more rapidly. As the flow pattern become developed (**Figure 4.2**) the flow become smooth and the velocity decreases almost linearly with the increasing fracture radius. It can be noted from the figure that lesser the overbalance pressure the lesser the frictional pressure loss in the near wellbore region i.e. within 2m of the wellbore.

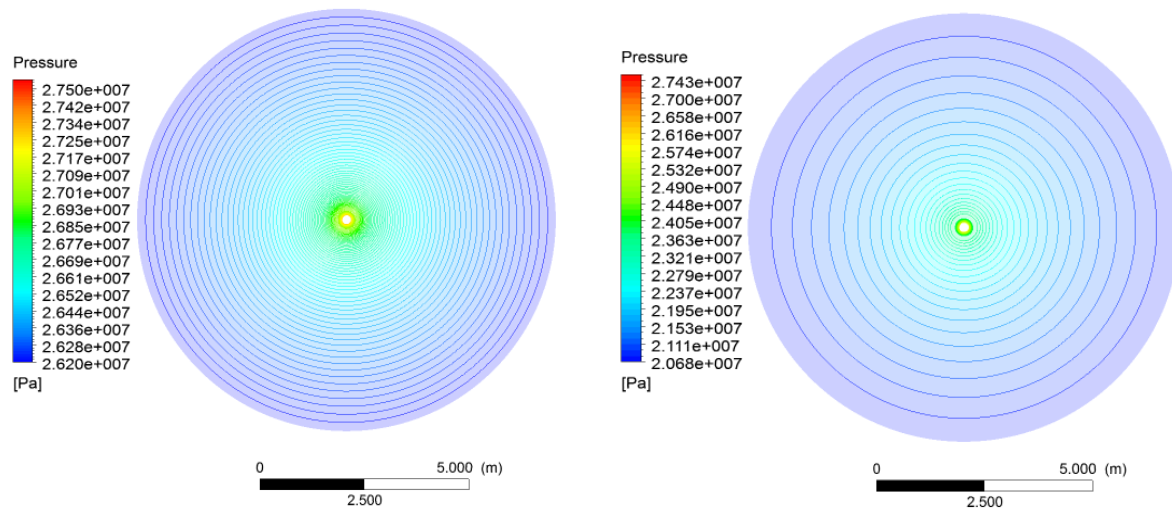**Figure 4.1: Pressure Contour: Left(Δp = 200 psi) and Right (Δp = 1000 psi)**
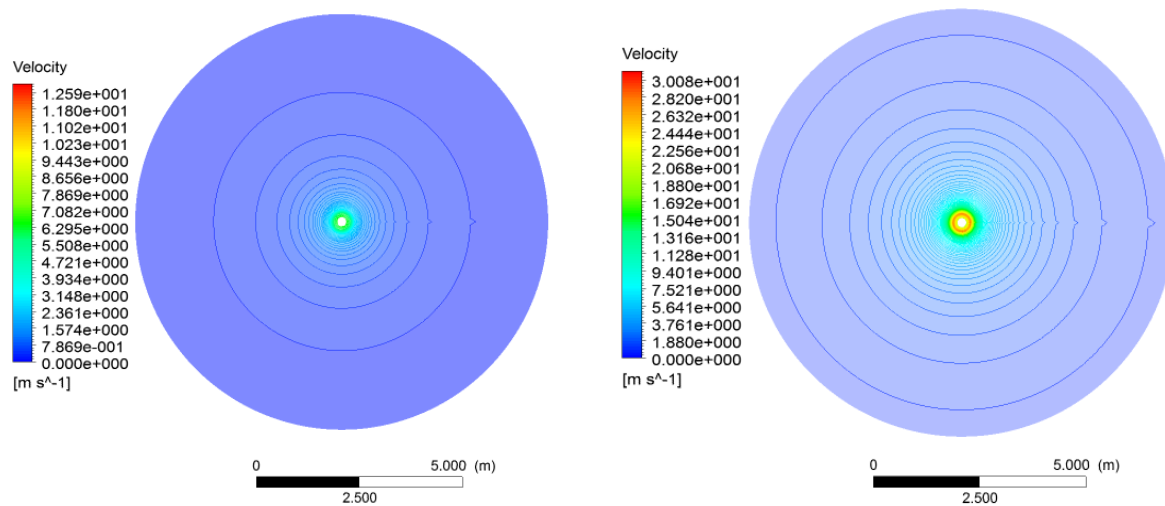
Figure 4.2: Velocity Contour: left (∆p =200psi) and Right (∆p =1000psi)

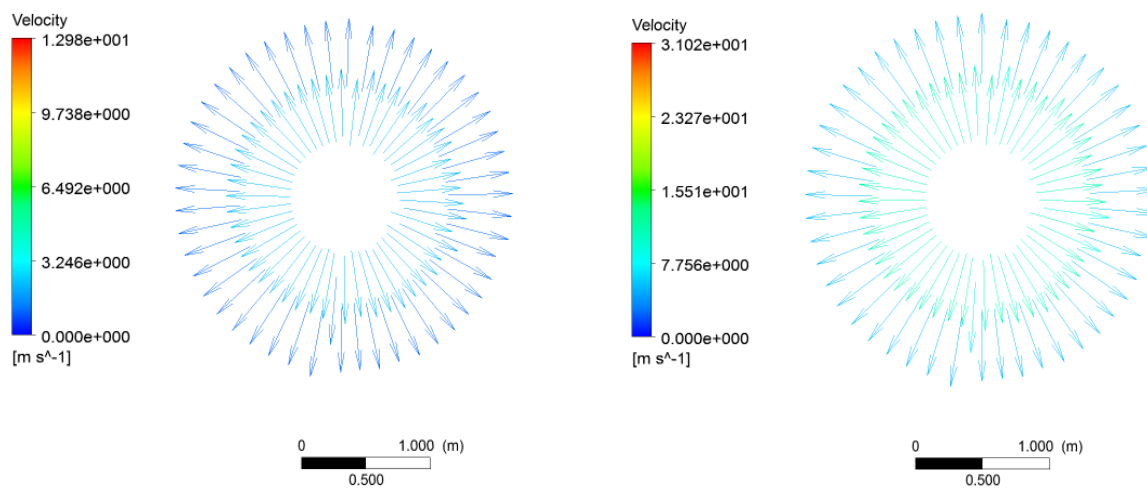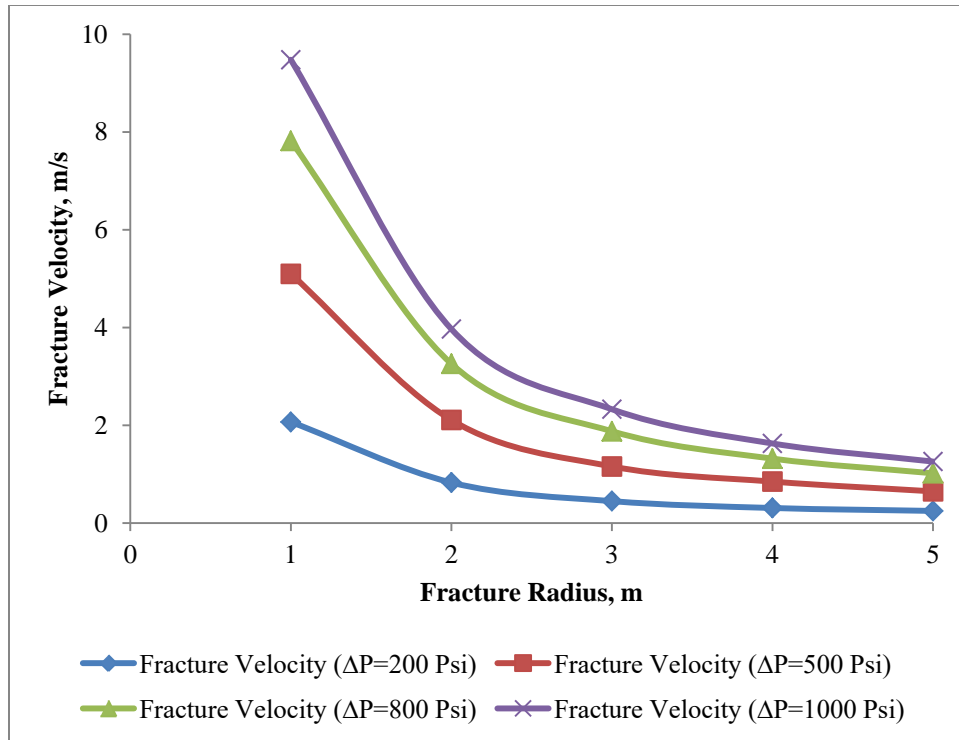**Figure 4.3: Velocity vector: left (∆p =200psi) and Right (∆p =1000psi)**

Figure 4.4: Drilling fluid velocity in smooth fracture at different fracture radius obtained from FLUENT

The trendline equations for four different lines from top to bottom of the **Figure 4.4** are given by equation (3), (4), (5) and (6) respectively.

$$V_{Fracture} = 2.056R_i^{-1.34} \dots \dots \dots \dots \dots (25); \ R^2 \ = \ 0.997$$

$$V_{Fracture} = 5.069R_i^{-1.29} \dots \dots \dots \dots \dots (26); \ R^2 \ = \ 0.998$$

$$V_{Fracture} = 7.804R_i^{-1.27} \dots \dots \dots \dots \dots (27); \ R^2 \ = \ 0.999$$

$$V_{Fracture} = 9.458R_i^{-1.26} \dots \dots \dots \dots \dots (28); \ R^2 \ = \ 0.999$$

It is clear from the equations that power law exponent increases with the increasing overbalance pressure which means that velocity of the drilling fluid at a certain distance from the wellbore will be greater for a higher value of overbalance pressure comparing to the velocity of the drilling fluid at a lower overbalance pressure. Similarly, the constant term in the equation also increases with the increasing overbalance pressure.

In statistics, R^2 value defines how well an equation can predict a given data set. The closer the value is to 1, the better the accuracy. It can be seen from the equations that the R^2 value for all the four curves in **Figure 4.4** is almost 1. Therefore, it is reasonable to conclude that the equations are good enough to predict the values of velocity of drilling fluid at any fracture radius for an overbalance pressure of 200 Psi, 500 Psi, 800 Psi and 1000 Psi.

Rough Walled Fracture:

All of the study on lost circulation conducted so far assumed that the fracture is smooth walled while in real cases it is not. Fracture wall roughness can have a considerable effect on the flow of drilling fluid inside fracture. Therefore, fracture wall roughness is introduced in the CFD model to find out the effect of roughness on the flow behavior of drilling fluid. However, similar to the CFD model for smooth walled fracture, the fluid leakoff through the fracture wall is considered negligible. Simulations were carried out for different roughness height i.e 2E-05, 4E-05, 6E-05, 8E-05 and 1E-04 at different overbalance pressure (200 psi, 500 psi, 800 psi and 1000 psi) and the obtained velocity of the drilling fluid is plotted against respective fracture as shown in **Figure 4.5**. It can be seen from the figure that the curve shifts upward (i.e. velocity of the drilling fluid increases) with increasing overbalance pressure. Furthermore, the velocity in the near wellbore region decreases more rapidly than deep into the fracture as the overbalance pressure increases which is due to the fact that the disturbances in the flow is more intense in that region for a high overbalance pressure comparing to a lower one. As the invasion radius increases, drilling fluid flow becomes developed and the drop in velocity becomes linear.
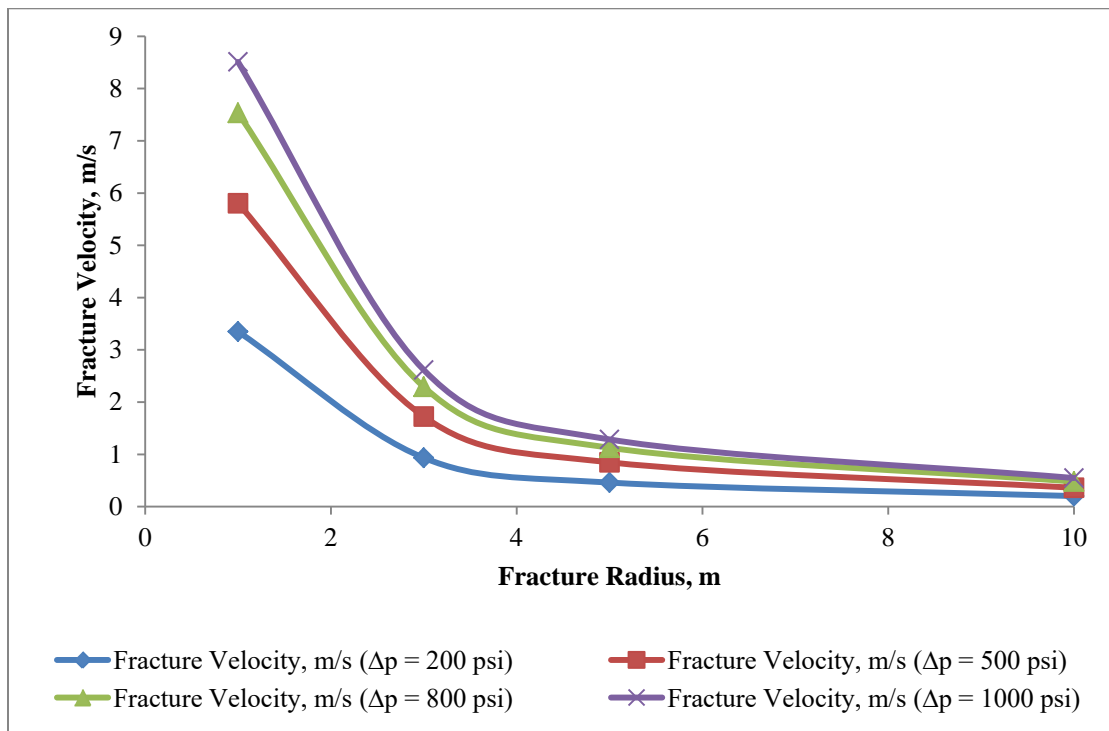

Figure 4.5: Drilling fluid velocity in rough fracture at different fracture radius obtained from FLUENT

The trendline equations for four different lines from top to bottom of the **Figure 4.5** are given by equation (29), (30), (31) and (32) respectively.

$$V_{Fracture} = 8.888R_i^{-1.18} \dots \dots \dots \dots (29); \ R^2 \ = \ 0.997$$

$$V_{Fracture} = 7.851R_i^{-1.19} \dots \dots \dots \dots (30); \ R^2 \ = \ 0.997$$

$$V_{Fracture} = 6.02R_i^{-1.20} \dots \dots \dots \dots (31); \ R^2 \ = \ 0.998$$

$$V_{Fracture} = 3.408R_i^{-1.22} \dots \dots \dots \dots (32); \ R^2 \ = \ 0.999$$

It can be noted from the equations that similar to the smooth walled fracture, for rough fracture, power law exponent and the co-efficient also increases with the increasing overbalance pressure. As the value of R^2 for all the four curves in **Figure 4.5** is close to 1; Hence, for the stated fluid properties in **Table 1.1**, by using those equations, for an overbalance pressure of 200 Psi, 500 Psi, 800 Psi and 1000 Psi; the velocity of drilling fluid at any fracture radius can be estimated.
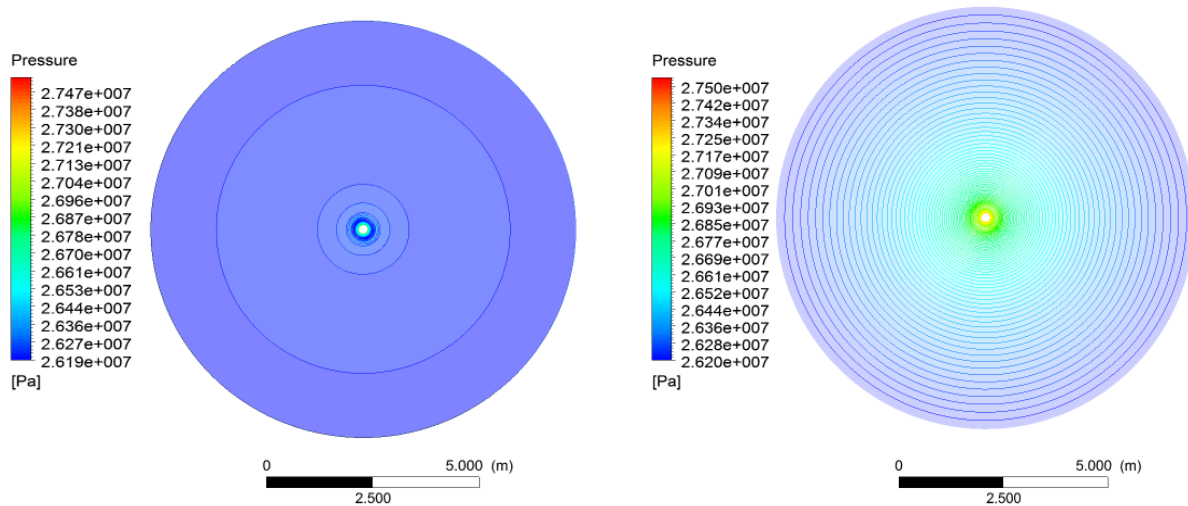

Figure 4.6: Pressure contour: Left (Rough Fracture: Roughness Height = 2E-05) and Right (Smooth Fracture)

The comparison between pressure drop in a rough fracture with a roughness height of 2E-05 m and a smooth walled fracture for an overbalance pressure of 200 psi is shown in **Figure 4.6**. It is clearly depicted in the figure that pressure drop is higher in a rough fracture compare to a smooth walled fracture. To be precise, for the stated overbalance pressure and roughness height, the difference between the pressure drop in a rough and a smooth walled fracture is found to be approximately 5 psi. In addition, considering the similar parameters, a comparison between the velocity in a rough and a smooth walled fracture is shown in **Figure 4.7**.It is obvious from the figure that the velocity in a smooth walled fracture is approximately 0.5 ms^{-1} higher than a rough

walled fracture. If fracture wall roughness is not considered, this discrepancy in pressure drop and velocity will led to an overestimation of invasion radius and mud loss volume. Therefore, for better accuracy it is necessary to consider fracture wall roughness.
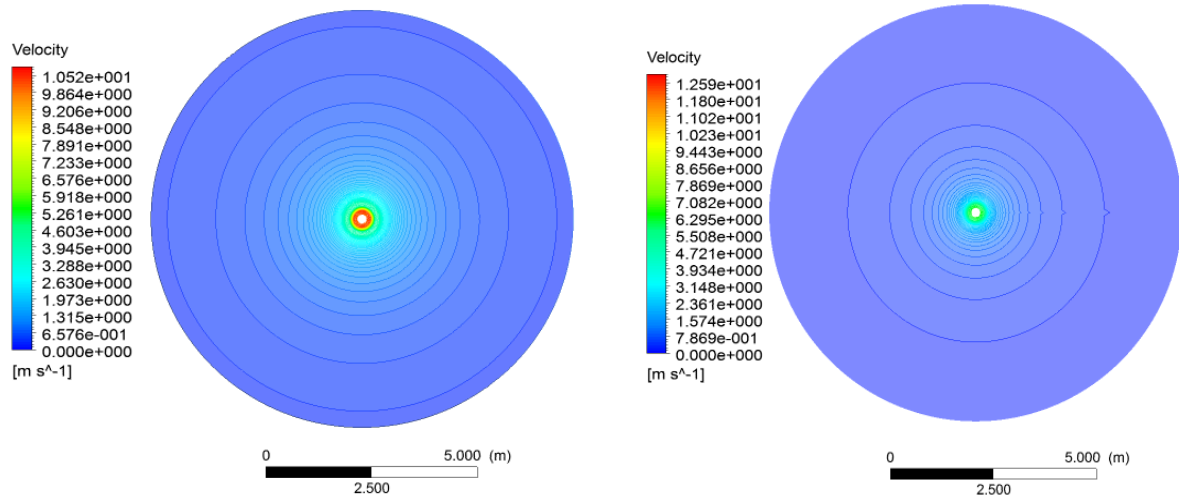

Figure 4.7: Velocity contour: Left (Rough Fracture) and Right (Smooth Fracture)
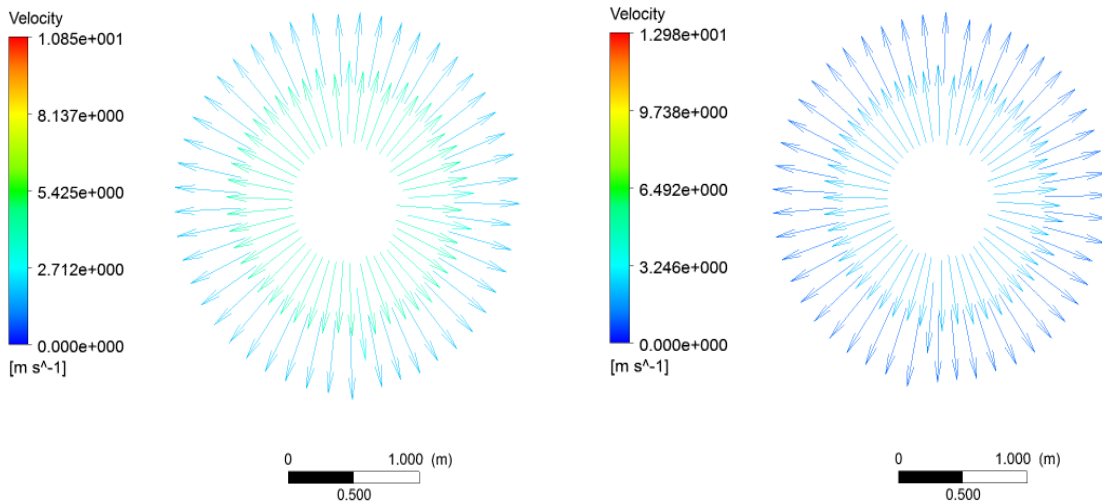

Figure 4.8: Velocity vector: left (Rough Fracture) and Right (Smooth Fracture)

Chapter Five: Discussion

Smooth Walled Fracture:

As the present study is based on the YPL type drilling fluid, to validate it, a scientifically valid model for flow of YPL type drilling fluid inside fracture is required. Therefore, the model proposed by Majidi et al. (2008) is selected because the model was proved to be correct when implemented during a drilling operation at a field owned by British Petroleum (BP). According to the study conducted by Majidi et al. (2008), the velocity of yield power law drilling fluid inside fracture can be calculated by the following equation-

$$\frac{dr_i}{dt} = \frac{(1-m)^{\frac{1}{m}}\{\frac{m}{2m+1}\left(\frac{w}{2}\right)^{1+\frac{1}{m}}\}\{\Delta P - \left(\frac{2m+1}{m+1}\right)\left(\frac{2\tau_y}{w}\right)(r_i - r_w)\}^{\frac{1}{m}}}{r_i\{k(r_i^{1-m} - r_w^{1-m})\}^{\frac{1}{m}}} \ldots \ldots \ldots \ldots \ldots (33)$$

Where m is the flow behavior index, w is the fracture width, k is the consistency index, r_i is the invasion radius, r_w is the wellbore radius, τ_y is the yield stress and Δp is the overbalance pressure

The results obtained from the equation above and the simulation results are compared in **Figure 8**. It is visible from the comparison that simulation results are close to the analytical results. As the overbalance pressure increases, the curves generated by the simulation results shift slowly towards left in the near wellbore region i.e. when the fracture radius is less than or equal to 2m mainly due to the initial turbulence. It is important to note that the velocity of drilling fluid decreases rapidly within 2 meter of the fracture radius because as the drilling fluid enters into a fracture, the flow of drilling fluid become turbulent in that region, hence, viscous forces among the layer of the drilling fluid cause to lose its energy abruptly. Whereas, beyond that region laminar flow pattern exist that is why velocity decreases more smoothly with the increasing invasion radius. Eventually, the drilling fluid will cease to flow when the driving energy is unable to overcome the yield stress of the fluid. The velocity of drilling fluid inside fracture is directly related to the overbalance pressure. If the overbalance pressure is high, the velocity of the drilling fluid will be higher. On the other hand, if the overbalance pressure is low, the velocity of the drilling fluid will be lower. It can be deduced from the effect of overbalance pressure on the velocity of the drilling fluid that the lower the velocity of drilling fluid, the lower will be loss of drilling fluid inside fractures. Therefore, in controlling the lost circulation, the overbalance pressure plays an important role. By decreasing overbalance pressure and keeping it above the pore pressure of the formation, the lost circulation can be mitigated.

However, controlling lost circulation is not an effective solution as costly mud will be lost into the fracture to some degree which may damage the formation. The effect may not be notable if the fracture width is small enough. Whereas, if the fracture width is big, the amount of mud lost

may be great enough to create an unstable situation in the wellbore as the hydrostatic pressure in the wellbore will be decreased due to lost circulation. Therefore, to avoid any kind of undesirable circumstances resulted from this phenomenon, when lost circulation begins, it is necessary to stop it as soon as possible by adding lost circulation materials (LCM) to the drilling mud. However, determining proper size of LCM materials to stop lost circulation is a challenging task as it depends on the fracture width. If the fracture width can be estimated at the beginning of lost circulation, the LCM equivalent to the fracture width can be added to the drilling mud which will block the fracture and the lost circulation will be stopped almost instantaneously.

The main purpose of the study is to find a way to determine the fracture width as soon as the lost circulation begins so that a proper treatment plan can be facilitated by selecting appropriate particle size of LCM. Prior to onset of drilling operation, few simulations like this study can be carried out so that a relation between mud loss rate and fracture width can be developed. Once the correlation is developed, the fracture width can be estimated from the mud loss rate instantaneously.
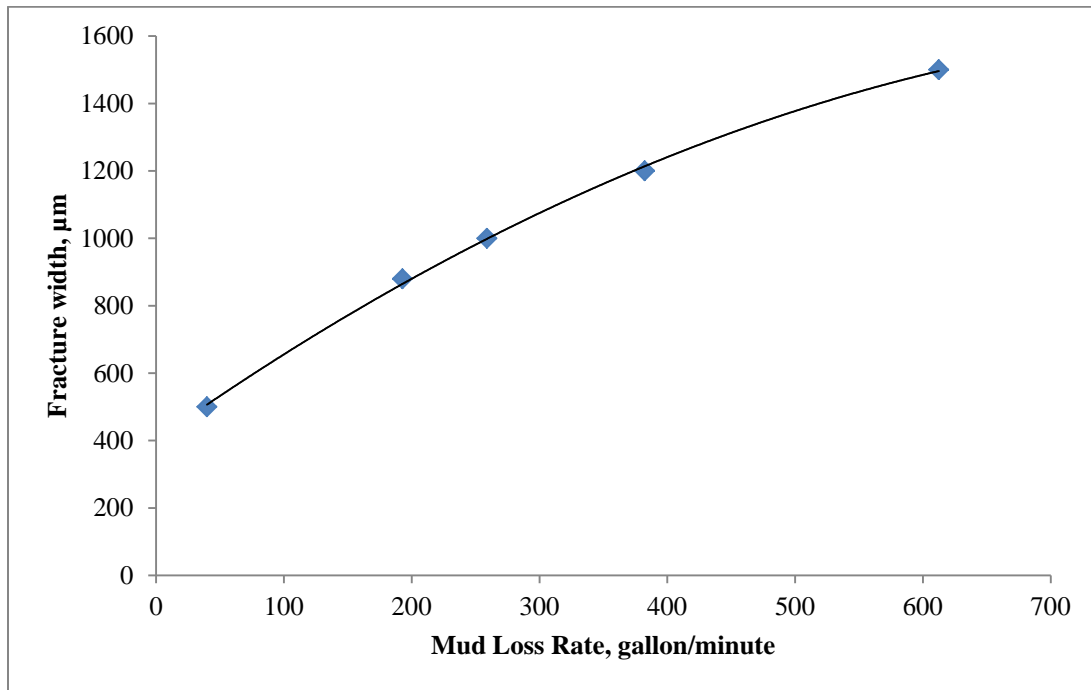

Figure 5.1: Relationship between fracture width and mud loss rate (when Δp= 500 psi)

The mud loss rate at different fracture width calculated using the stated parameters in table 1 and then the values were plotted in **Figure 5.1** find out a relation between fracture width and mud loss rate. It can be noted from the figure that mud loss rate increases non-linearly with the increasing fracture width. The trendline equation for **Figure 5.1** is given by-

$$w = -0.001q^2 + 2.682q + 401.9 \dots\dots\dots\dots\dots (34); R^2 = 0.999$$

Where w and q is fracture width and mud loss rate respectively

Therefore, prior to onset of drilling, by knowing mud rheological parameters from the mud report and conducting a few simulations similar correlations like **Equation 34** can be constructed to estimate the fracture width from the mud loss rate.

Additionally, when the lost circulation is stopped by adding proper LCM, it is necessary to determine the invasion radius of drilling mud so that a proper treatment plan can be facilitated during well development stage. Similar correlation like equation 17 can be developed by analyzing the data. The fracture velocities obtained from the equation 7 and the simulations are compared in **Figure 5.2**.
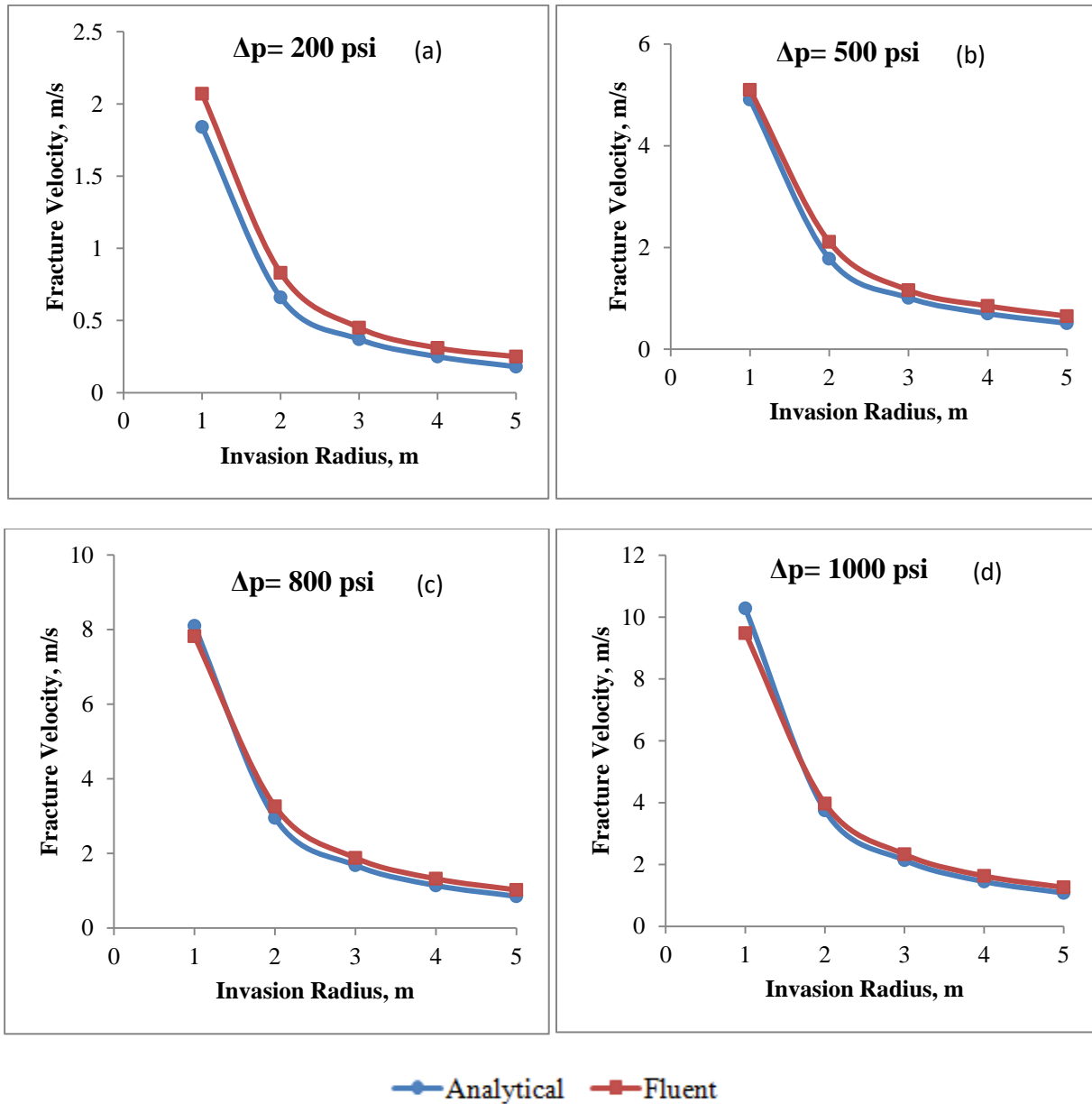

Figure 5.2: Comparison between results obtained from analytical method and numerical simulations

The equation of best fitted line for **Figure 5.2(a), 5.2(b), 5.3(c) and 5.4(d)** are given by equation (9), (10), (11) and (12) respectively.

$$V_{Fracture} = 1.9R_i^{-1.4} \ldots\ldots\ldots\ldots (35); \; R^2 = 0.997$$
$$V_{Fracture} = 4.9R_i^{-1.4} \ldots\ldots\ldots\ldots (36); \; R^2 = 0.999$$
$$V_{Fracture} = 7.9R_i^{-1.4} \ldots\ldots\ldots\ldots (37); \; R^2 = 0.999$$
$$V_{Fracture} = 9.9R_i^{-1.4} \ldots\ldots\ldots\ldots (38); \; R^2 = 0.999$$

It can be seen from the best fitted line equations that the drilling fluid velocity inside fracture is a function of invasion radius. The drilling fluid velocity follows power law relation with the invasion radius which means the velocity of the drilling fluid decreases with increasing invasion radius. And the co-efficient in the right hand side of the equations is a function of overbalance pressure. As the overbalance pressure increases the value of the coefficient also increases. Therefore, it is logical to conclude that the velocity of the drilling fluid is a function of both the overbalance and the invasion radius. Denoting the co-efficient as K, it can be generalized that the velocity of drilling fluid inside fracture is:

$$V_{Fracture} = KR_i^{-1.4} \ldots\ldots\ldots\ldots (39)$$

The values of K with corresponding overbalance pressure are summarized in the following table:

Table 5.1: Values of co-efficient at different overbalance pressure

Overbalance Pressure (Δp), Psi	Co-efficient, K (Analytical)	Co-efficient, K (Fluent)	Co-efficient, K (Best Fitted)
200	1.819	2.056	1.9
500	4.82	5.069	4.9
800	7.964	7.804	7.9
1000	10.11	9.458	9.9

Plotting these values of K against corresponding overbalance pressure, it is found that K changes linearly with increasing overbalance pressure (**Figure 5.3**). As the value of overbalance pressure increases, value of the co-efficient K also increases.
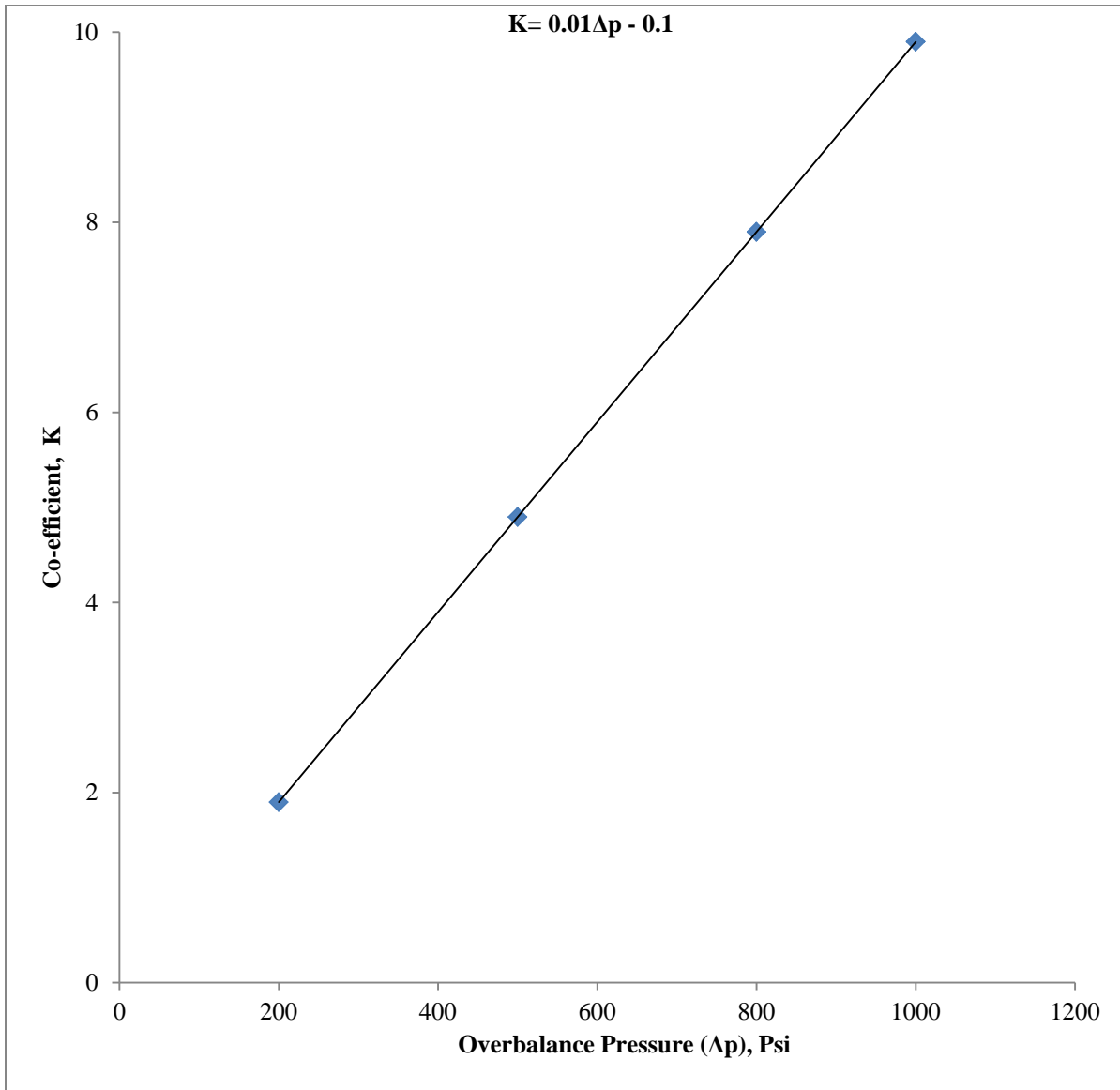
Figure 5.3: Effect of Overbalance pressure on co-efficient K

Therefore, it can be generalized that when consistency index is 0.004 kg/m-s, flow behavior index is 0.94, Yield stress is 4.022 Pascal and the fracture width is 880µm, the velocity of drilling fluid inside fracture can be calculatedusing the following correlation:

$$V_{\text{Fracture}} = (0.01\Delta P - 0.1)R_i^{-1.4} \dots \dots \dots \dots \dots (40)$$

After completing the study, to validate the correlation, the results produced by the correlation are compared with analytical results obtained from the model developed by Majidi et al. (2008) and fluent simulation results in **Figure 5.4**. This comparison shows that the results obtained by the correlation are in close match with the analytical results and the numerical simulation results.
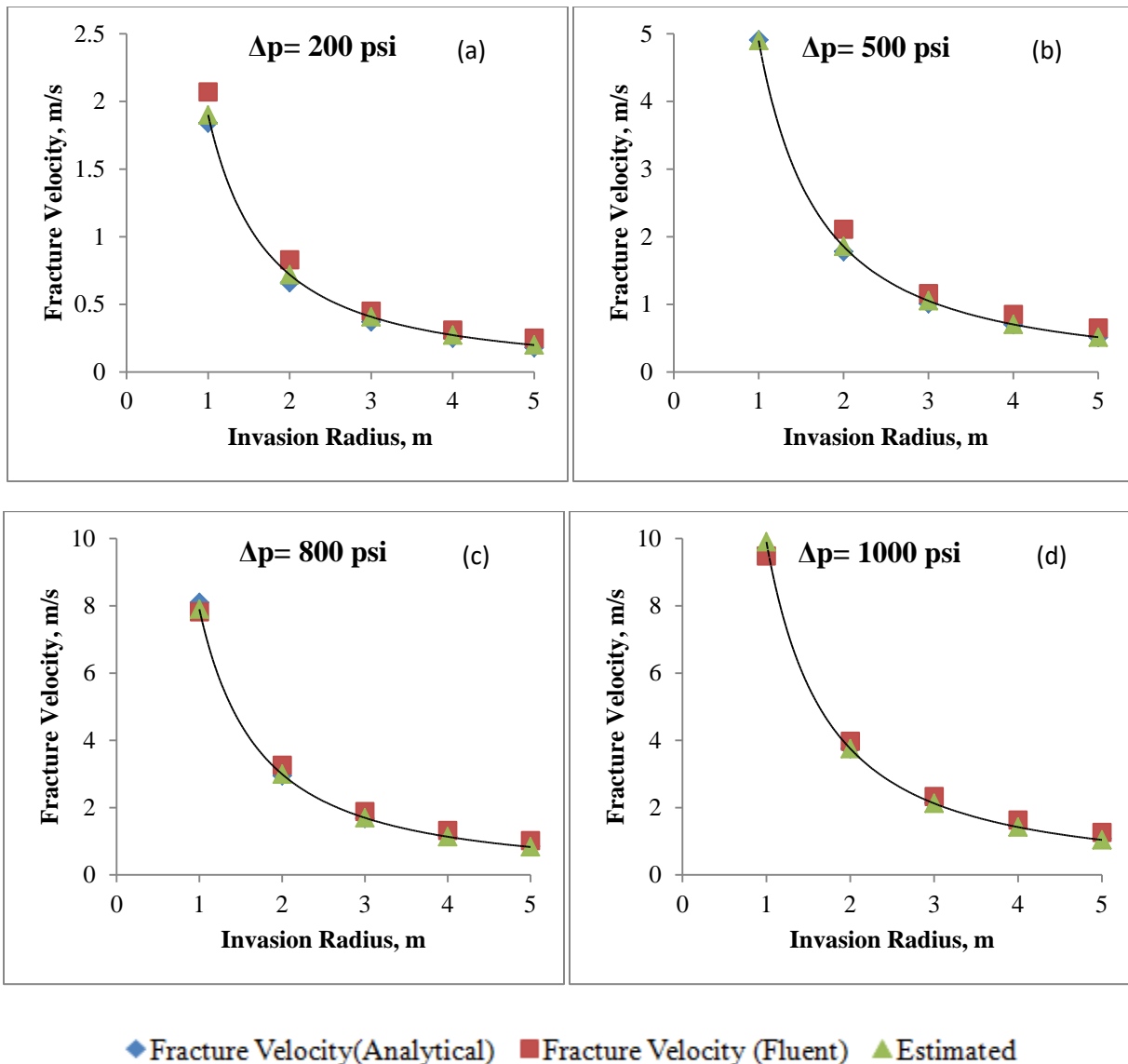
Figure 5.4: Comparison among the values obtained by the correlation, analytical method and numerical simulations

One of the drawbacks in this CFD analysis is that FLUENT over-predicts the value of drilling fluid velocity than the velocity values obtained from the analytical method. However, as the overbalance pressure increased to 800 Psi, FLUENT starts to under-predict the drilling fluid velocity when invasion radius is less than 1m. The percentage of deviation of the numerical simulation results and the correlation results from the analytical results are plotted in **Figure 5.5**. From **Figure 5.5 (Left)**, it is clear that the error in the numerical simulation decreases with increasing overbalance pressure, however, the error increases with increasing invasion radius. Therefore, for a high overbalance pressure, the simulation will produce more accurate result in the near wellbore region. The closer the distance from the wellbore, the more accurate the simulation will be.
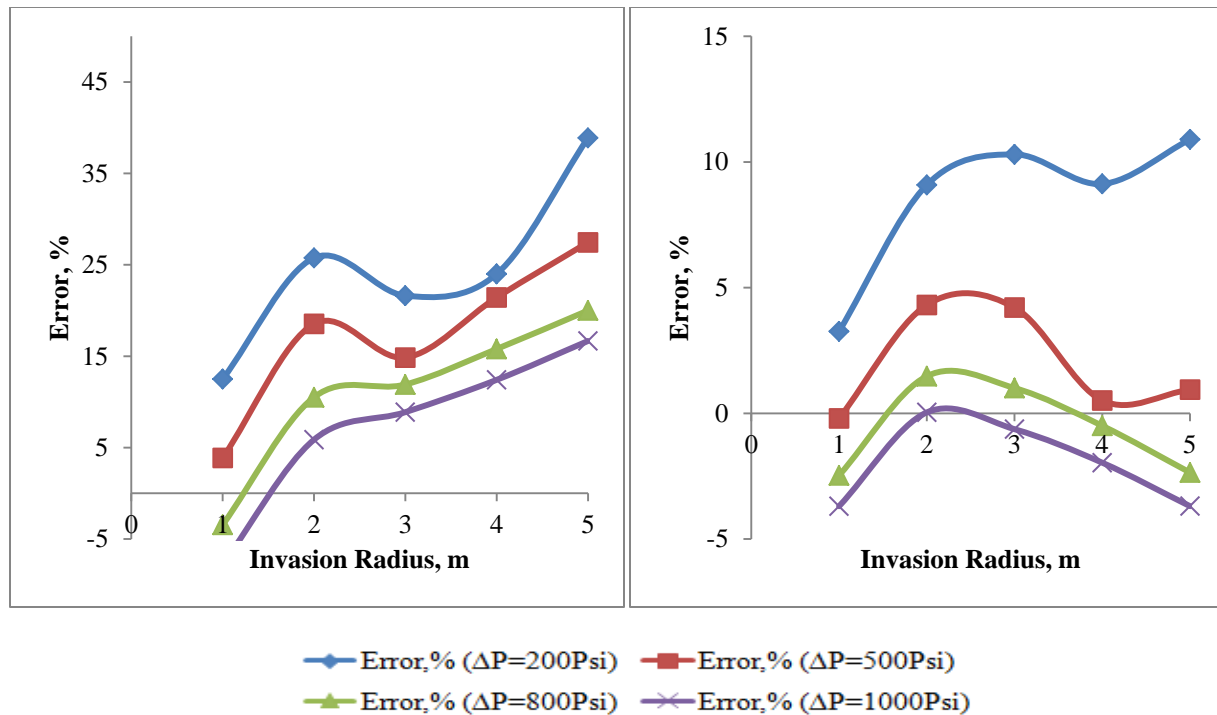
Figure 5.5: Deviation of simulation results from analytical method (Left) and Deviation of correlation results from analytical method (Right)

In addition, the percentage of deviation of the results obtained using the correlation from the analytical results is plotted in **Figure 5.5 (Right)**. It can be seen from the figure that the correlation produce less error than the numerical simulation. The error produce in the numerical simulation is ranges from -10% to +39%, whereas, the error produce using the correlation ranges from -3% to +10%. The error in the correlation results start to decrease as the overbalance pressure is increased from 200 Psi. Among the four overbalance pressure, the correlation produce more accurate results for overbalance pressure of 500 Psi, 800 Psi and 1000 Psi. It is clearly depicted in the figure that in those cases, the error is decreased to ±3%.

Moreover, results obtained from the equation and the correlation is compared in **Figure 5.6** to find out the deviation between them. The closer the slope of the plot to 1, better the approximation. It is visible from the figure that the slope is almost 1 which proves that the approximation is good enough.
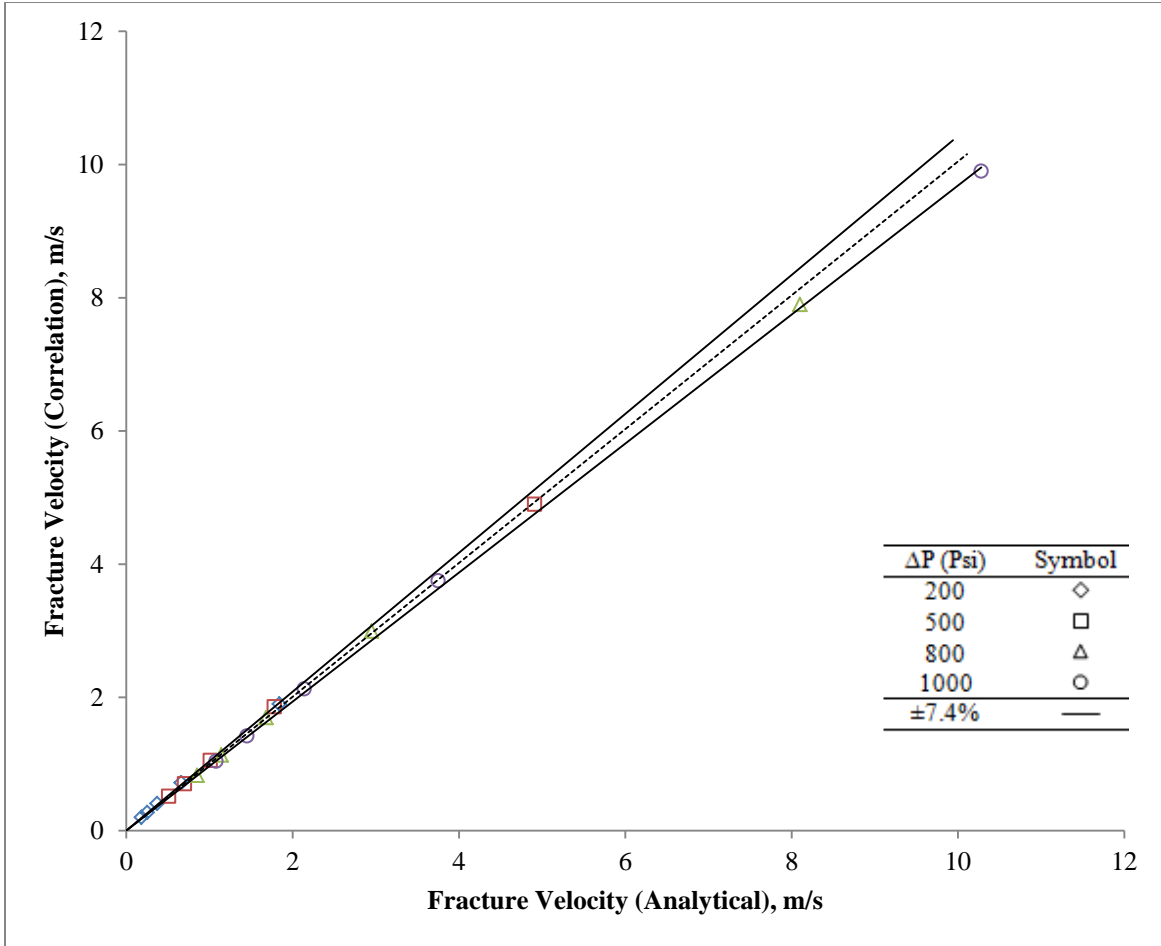
Figure 5.6: Comparison between analytical results and correlation results

Recalling the basic equations to calculate flow rate and mud loss volume:

$$q = 2\pi R_i W * V_{Fracture} \ldots \ldots \ldots \ldots \ldots (41)$$

$$V = q * t \ldots \ldots \ldots \ldots \ldots (42)$$

Assuming drilling fluid was lost into the fracture at a constant rate, for a fracture width of 880μm and stated fluid properties given in **Table 1,** the equation (12), 13) and (14) can be combined to determine the invasion radius from the total mud loss volume:

$$R_i = [\frac{9.217 * 10^{-5}(0.01 * \Delta P - 0.1)t}{V}]^{2.5} \ldots \ldots \ldots \ldots \ldots (43)$$

Where

ΔP = Overbalance pressure, psi

t = Time, minute

V = Total mud loss volume, m^3

Rough Walled Fracture:

Understanding how fracture wall roughness affects the drilling fluid flow inside fractures is important when studying lost circulation. Usually, the natural fractures consist of surfaces with different order of roughness which has crucial effects on the drilling fluid flow behavior inside fractures. The theoretical and experimental works that are done so far on lost circulation considered the fracture wall as smooth which is not realistic to assume; whereas, the velocity of the drilling fluid inside fracture will vary depending on the value of roughness height. When the value of roughness height is higher, the pressure drop across the fracture radius will be higher; consequently, the drop in drilling fluid velocity will be higher. While for a fracture with low roughness height both the value of pressure drop and the reduction in velocity will be lower. Considering those facts, fracture wall roughness is introduced into the developed CFD model to better comprehend the effect of fracture wall roughness on the flow behavior of the drilling fluid inside natural fractures. The simulation was carried out for a fracture height of 2E-05 m, 4E-05 m, 6E-05 m, 8 E-05 m, 1E-04 m and the results obtained for different overbalance pressure of 200 psi, 500 psi, 800 psi and 100 psi were compared with the results obtained from a smooth walled fracture in **Figure 5.8 (a), 5.8 (b), 5.8 (c), 5.8 (d) and 5.8 (e)** respectively. Those figures show that as the overbalance pressure and invasion radius increases, the effect of roughness on the drilling fluid velocity becomes more prominent i.e. decreases more rapidly than that of a smooth walled fracture.

The mud loss rate at different fracture width is estimated using the average drilling fluid velocity inside a rough fracture obtained from the simulation when the invasion radius is 5m, roughness height is 2E-05 m and the overbalance pressure is 1000 psi. The values of mud loss rate were plotted against respective fracture width in **Figure 5.7**. The trendline equation for **Figure 5.7** is given by:

$$w = 0.00013q^{0.33} \ldots \ldots \ldots \ldots \ldots (44); \ R^2 = 0.999$$

Where;

w = Fracture width, m

q = Mud loss rate, gpm (gallon/minute)

As the value of R^2 is close to 1, the equation is good enough to predict the value of fracture width from mud loss rate for the stated fluid properties given in **Table 3.1**. Similar correlation can be developed prior to onset of drilling knowing the mud properties, overbalance pressure and roughness height.
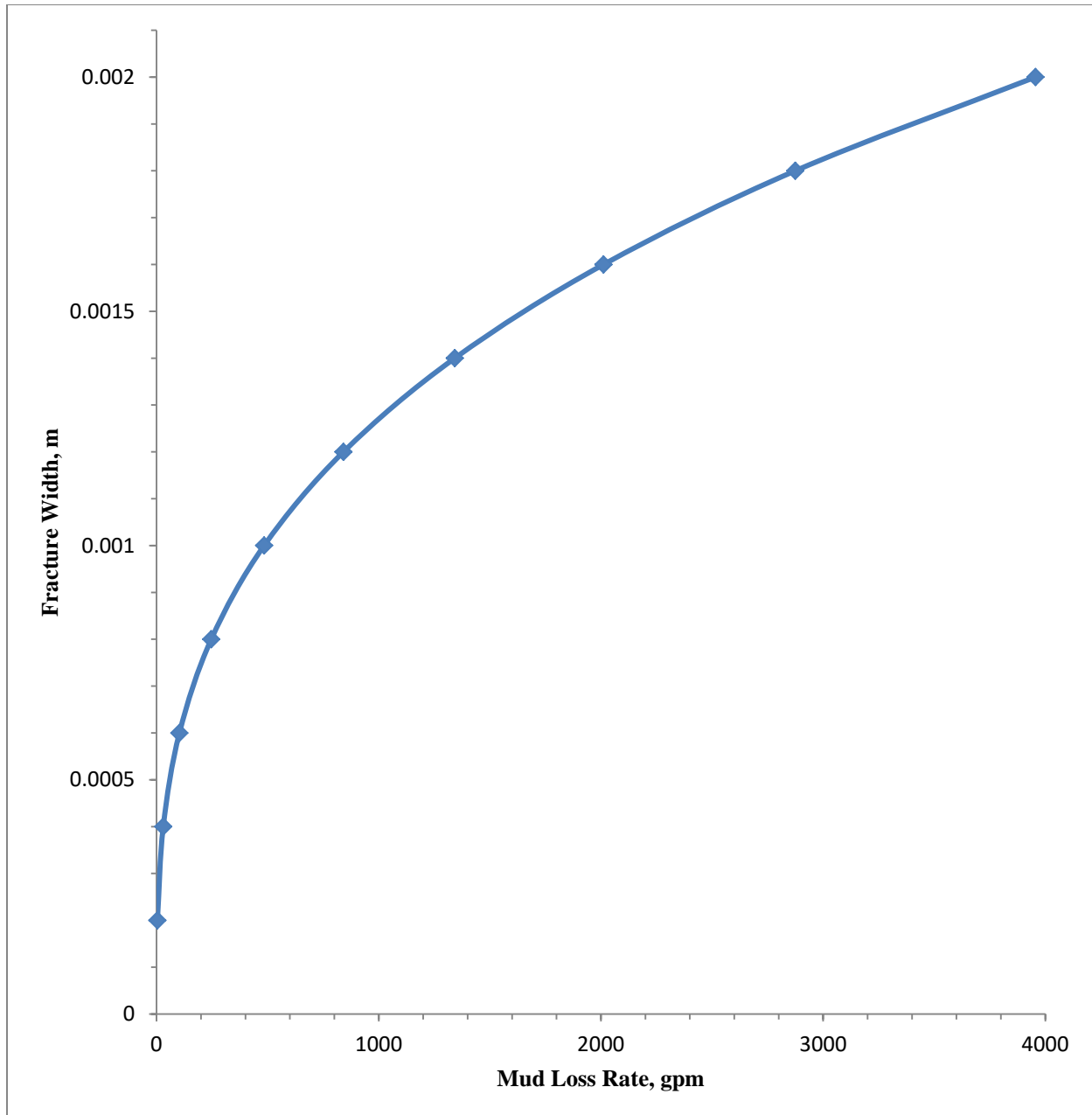
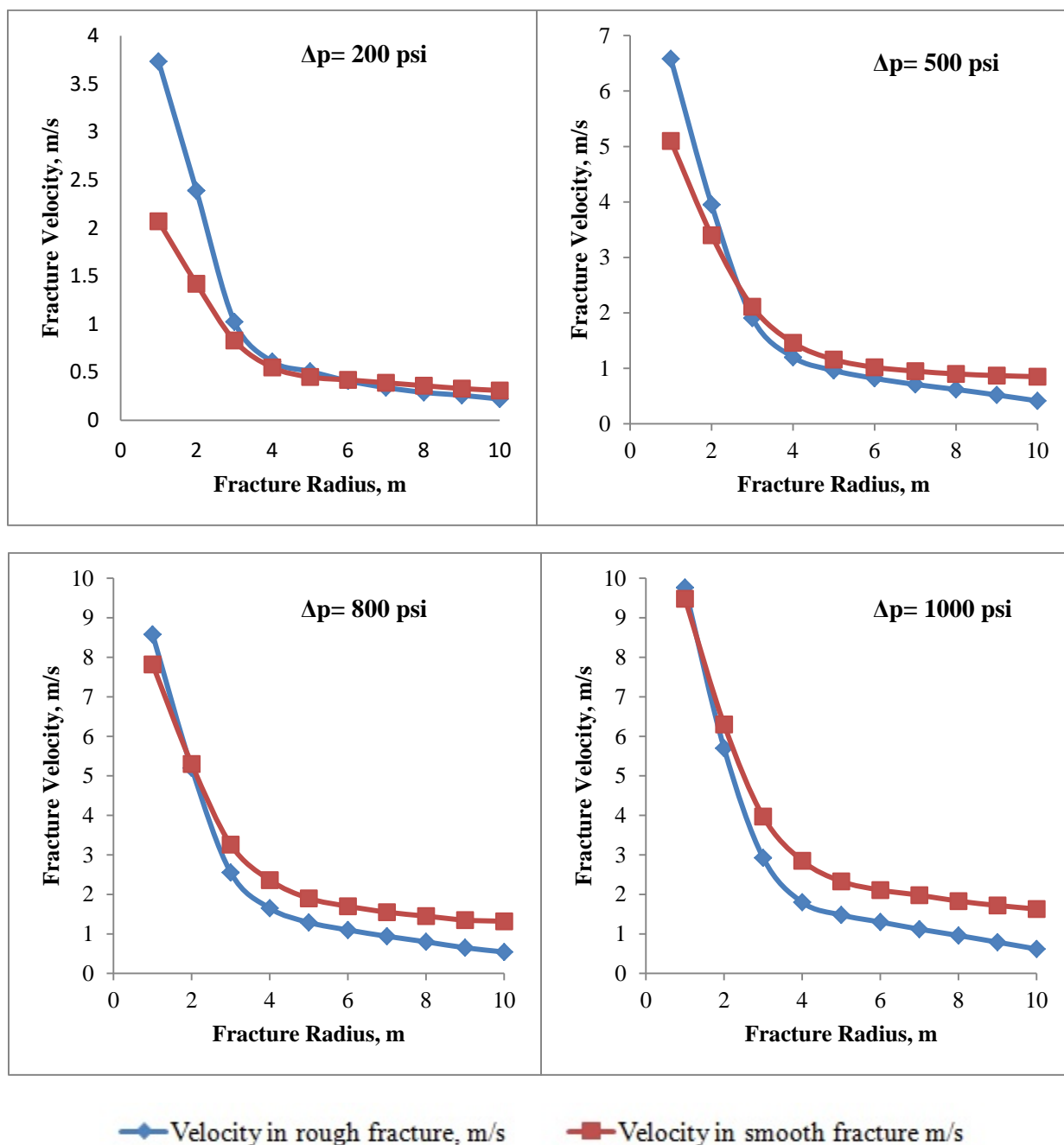**Figure 5.7: Relationship between fracture width and mud loss rate (when Δp= 1000 psi)**

Figure 5.8 (a): Comparison between velocities in smooth and rough fractures (Roughness Height =2e-05 m)
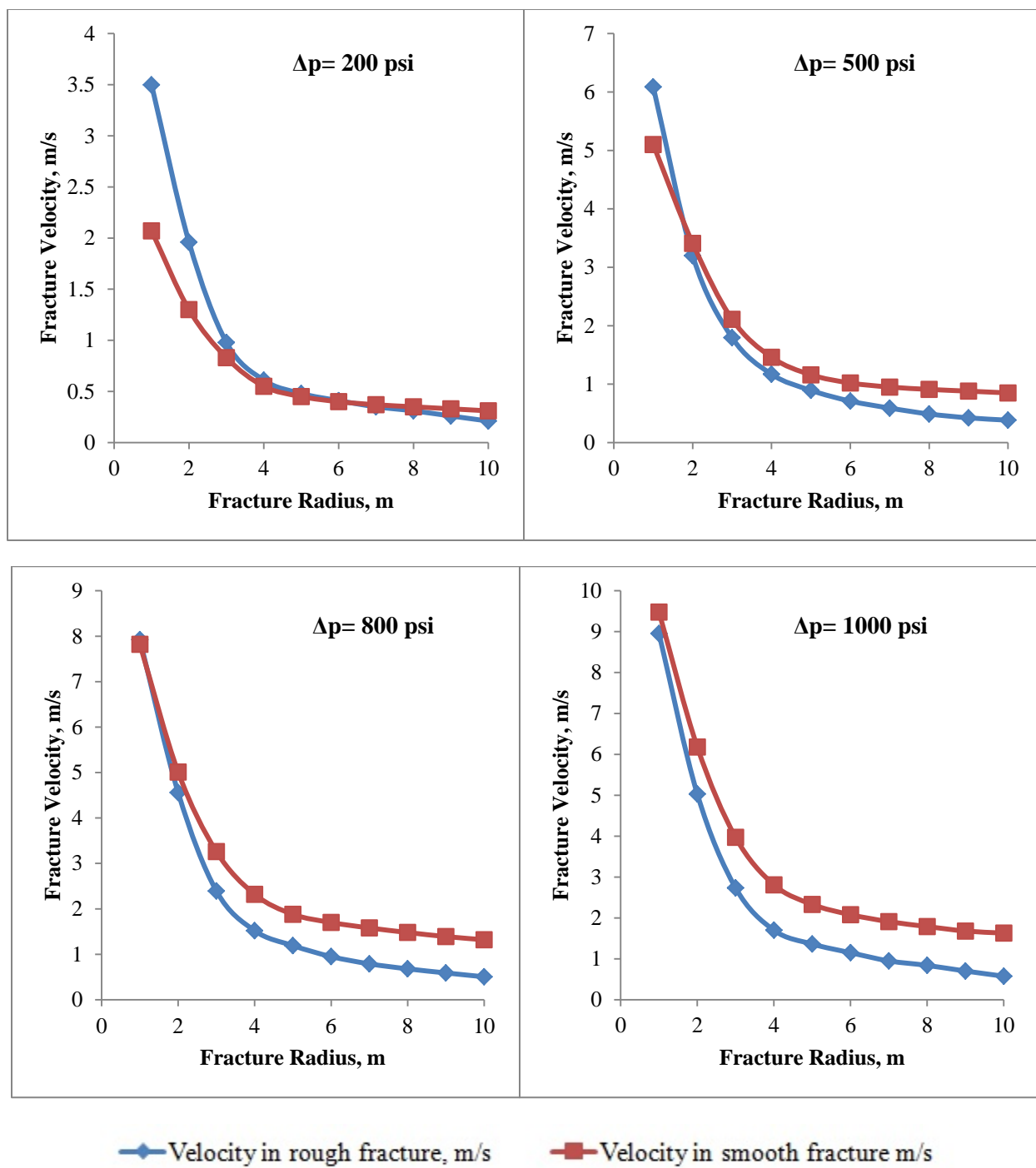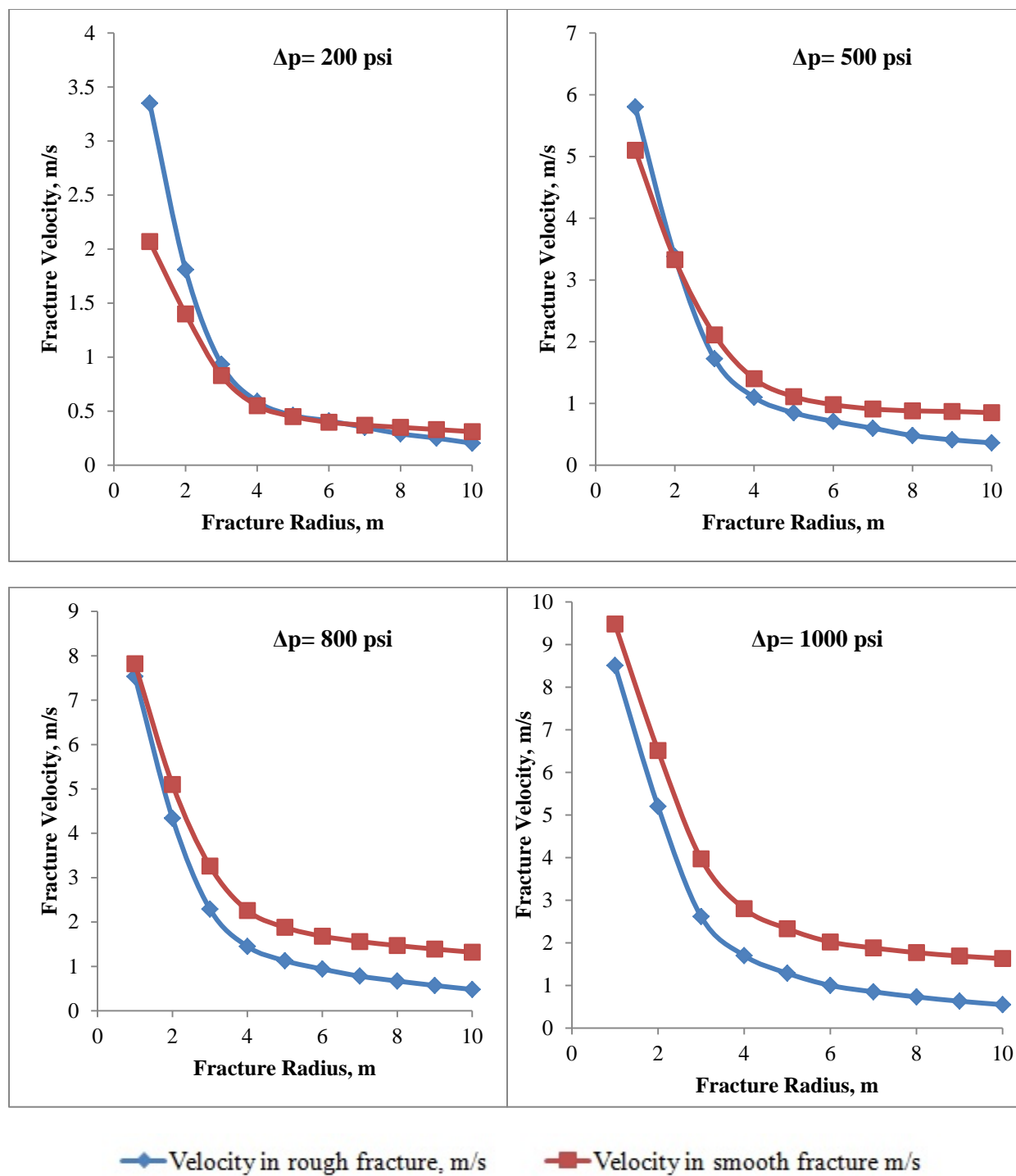
Figure 5.8 (b): Continued (Roughness Height =4e-05 m)

Figure 5.8 (c): Continued (Roughness Height =6e-05 m)

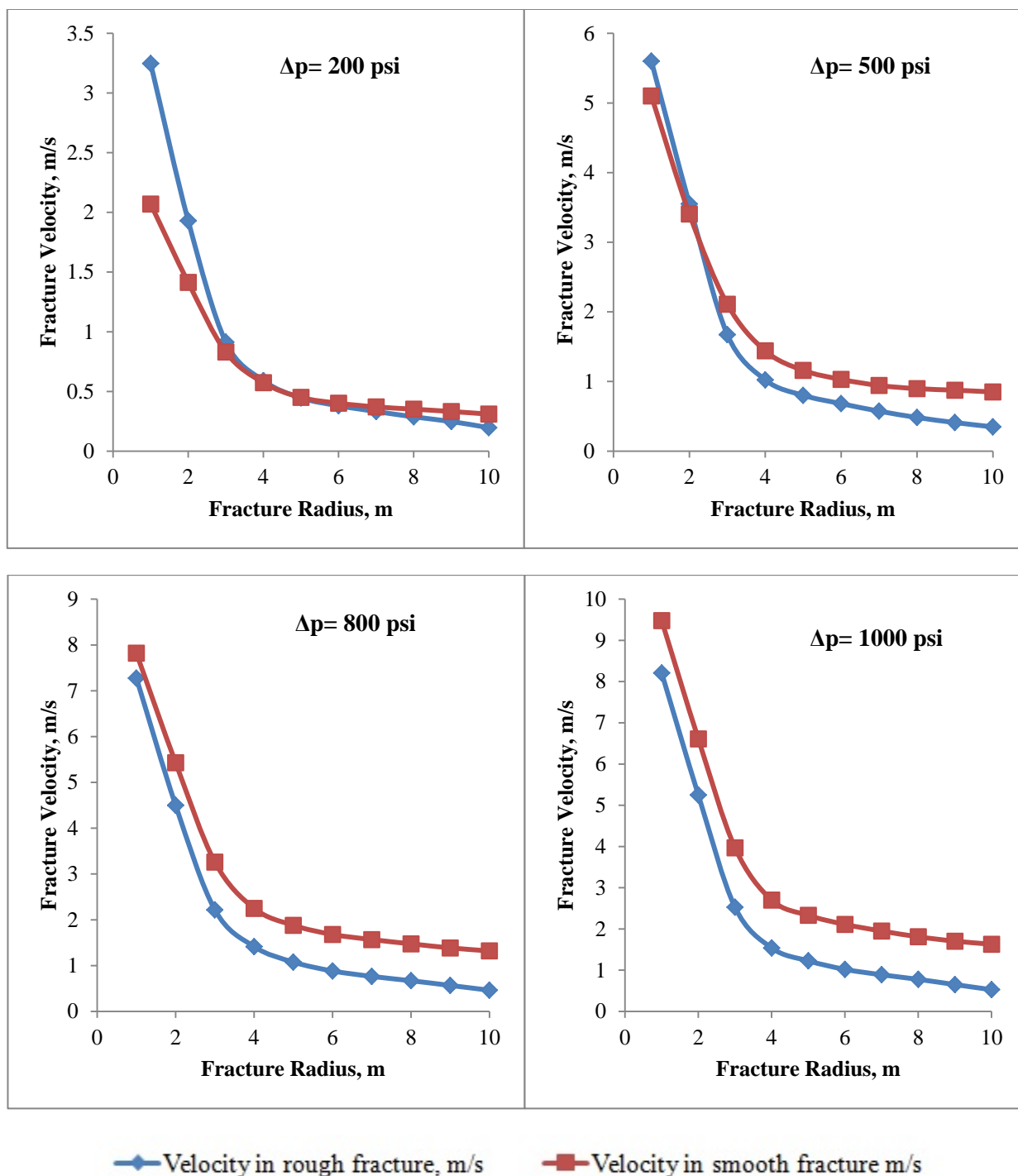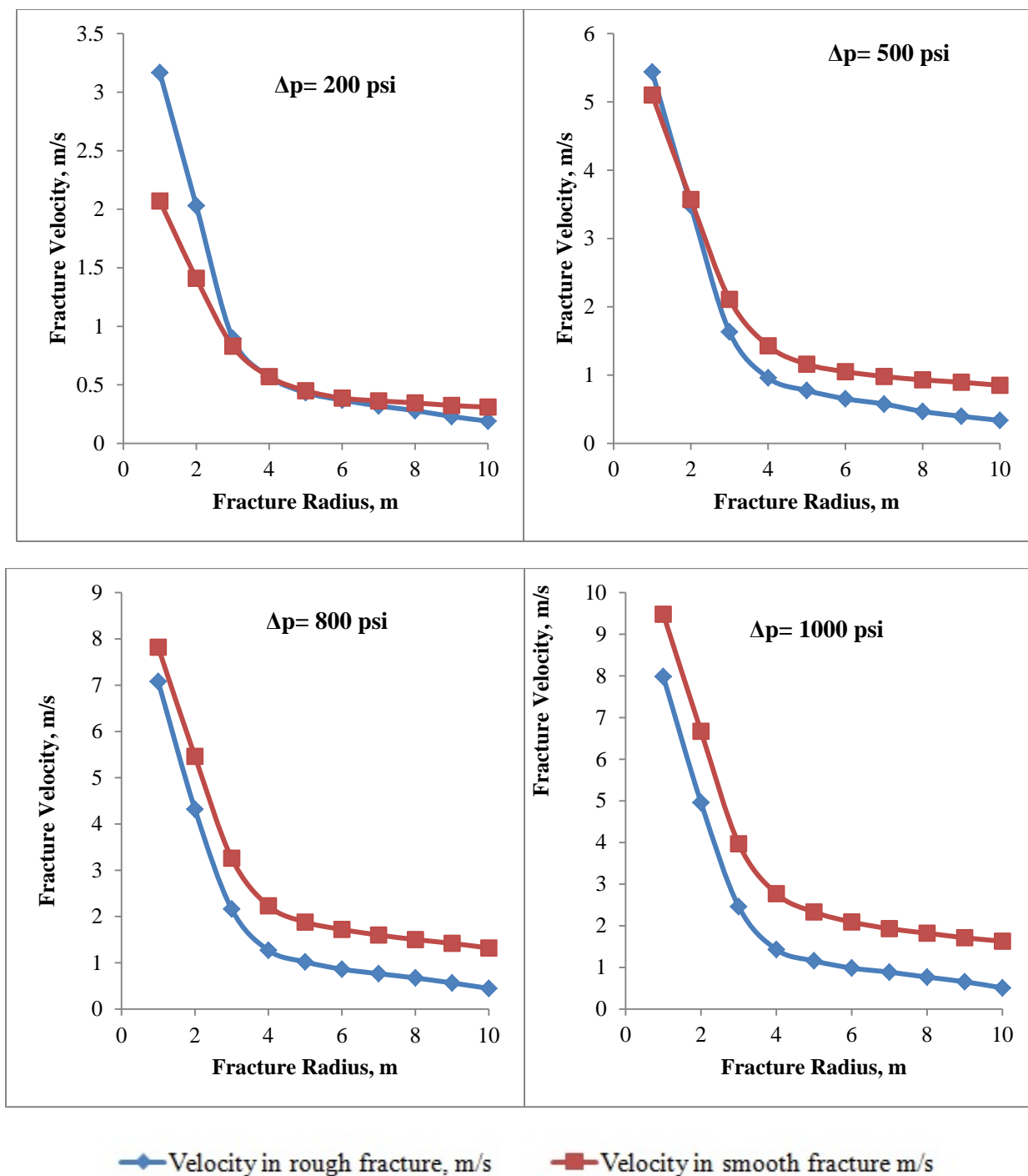**Figure 5.8 (d): Continued (Roughness Height =8e-05 m)**

Figure 5.8 (e): Continued (Roughness Height =1e-04 m)
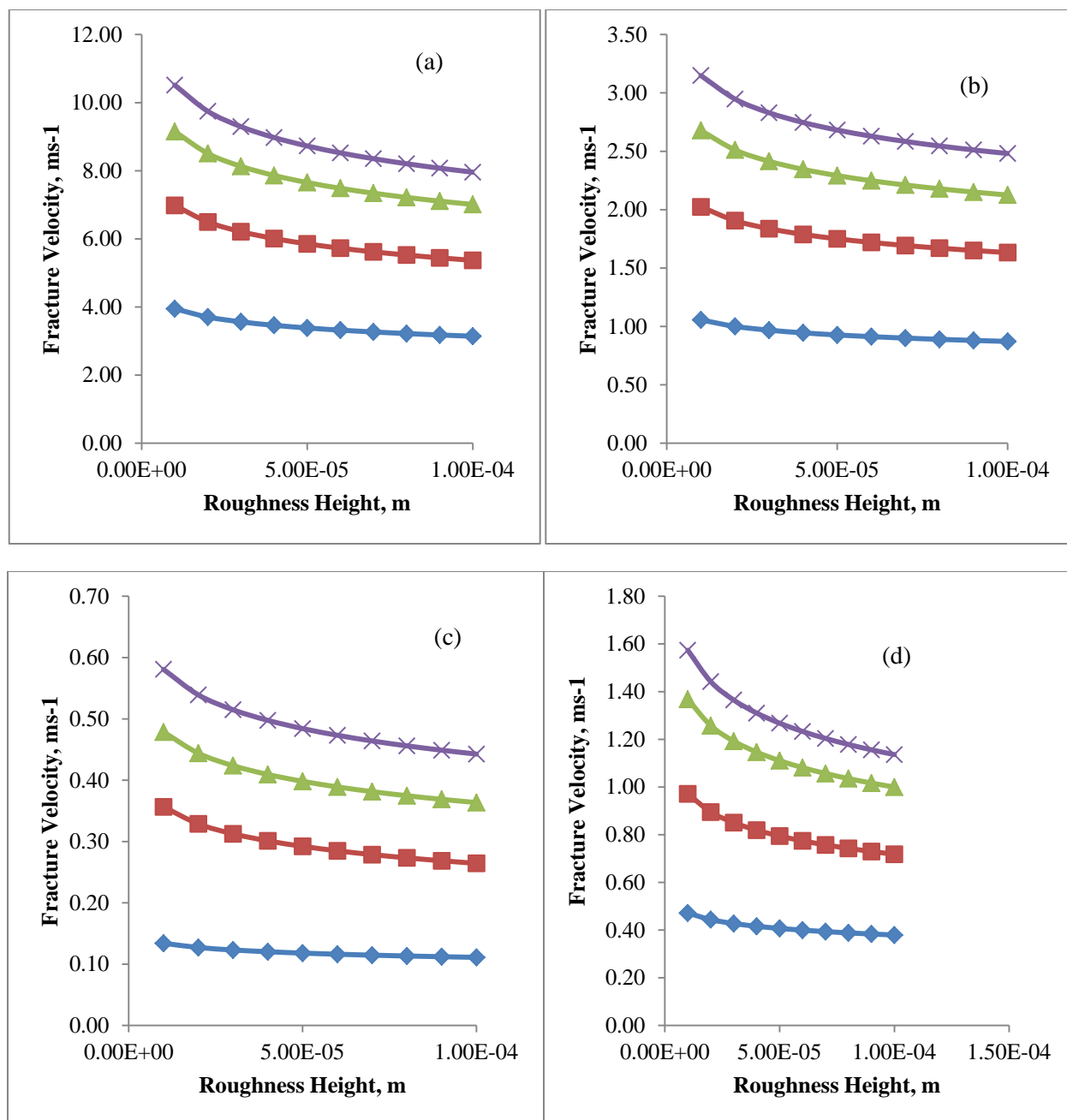
Fig 5.9: Effect of Roughness Height on Fracture Velocity: (a) when R_i= 1m, (b) When R_i= 3m, (c) When R_i= 5m, (d) When R_i= 10m

The trendline equations for **Figure 5.9** are given below:

Figure 5.9 (a)
v = -0.35ln(Rh) – 0.082; R² = 0.999
v = -0.70ln(Rh) – 1.078; R² = 1
v = -0.93ln(Rh) – 1.556; R² = 0.999
v = -1.11ln(Rh) – 2.265; R² = 0.999

Figure 5.9 (b)
v = -0.08ln(Rh) + 0.135; R² = 0.992
v = -0.17ln(Rh) + 0.067; R² = 0.999
v = -0.24ln(Rh) – 0.085; R² = 0.999
v = -0.29ln(Rh) – 0.19; R² = 0.999

Figure 5.9 (c)
v = -0.04ln(Rh) + 0.011; R² = 0.996
v = -0.11ln(Rh) – 0.295; R² = 0.99
v = -0.16ln(Rh) – 0.474; R² = 0.99
v = -0.19ln(Rh) – 0.614; R² = 0.988

Figure 5.9 (d)
v = -0.01ln(Rh) + 0.019; R² = 0.985
v = -0.04ln(Rh) – 0.104; R² = 0.999
v = -0.05ln(Rh) – 0.097; R² = 0.997
v = -0.06ln(Rh) – 0.11; R² = 0.997

It is clear from the trendline equations given above; the flow of drilling fluid inside a rough fracture follows a common trend. Thus, it can be generalized that velocity inside a rough fracture follows the following equation:

$$v = a \ln(Rh) + b \dots\dots\dots\dots\dots (45)$$

Where,

v = Drilling fluid velocity inside fracture, ms^{-1}

Rh = Roughness Height, m

a& b = co-efficient

It is interesting to note from the trendline equations that the co-efficient a and b decreases with increasing overbalance pressure. To find out a common relation between overbalance pressure and the co-efficients, value of a and b is plotted against respective overbalance pressure in **Figure 5.10 and 5.11**.
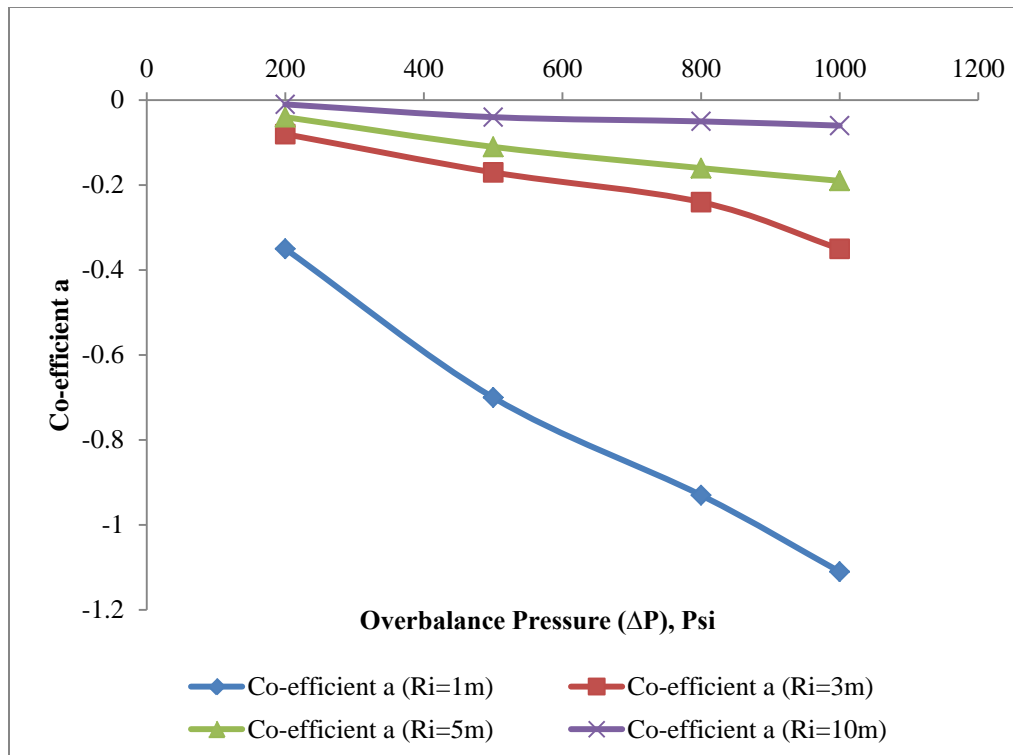
Fig 5.10: Effect of Overbalance Pressure on Coefficient "a"
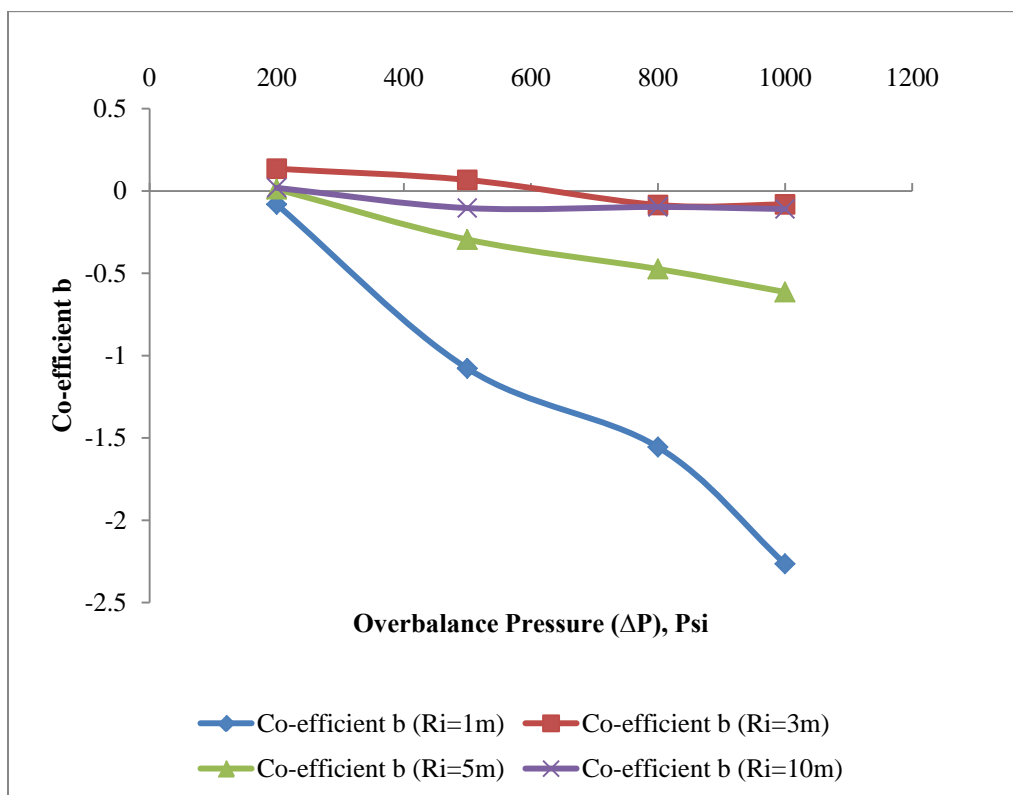
Fig 5.11: Effect of Overbalance Pressure on Coefficient "b"

The trendline equations of co-efficient a and b plotted in above figure is given by:

When R_i = 1m:

a = -0.1896 – 0.000933*ΔP
b = 0.374 – 0.002591*ΔP

When R_i = 3m:

a = -0.0365 – 0.000250*ΔP
b = 0.2424 – 0.000419*ΔP

When R_i = 5m:

a = -0.00850 – 0.000186*ΔP
b = 0.1349 – 0.000765*ΔP

When Ri = 10m:

a = -0.00259 – 0.000060*ΔP
b = 0.0176 – 0.000145*ΔP

By looking at the equations given above, it can easily understood that co-efficients in the equations also follows a trend. Therefore, the generalized form of the co-efficient a and b is given by:

$$a = c + d * \Delta P \dots \dots \dots \dots \dots (46)$$

$$b = e + f * \Delta P \dots \dots \dots \dots \dots (47)$$

Table 5.2: Co-efficient c, d, e and f at different invasion radius

Invasion Radius, Ri (m)	Co-efficient c	Co-efficient d	Co-efficient e	Co-efficient f
1	-0.1896	-0.000933	0.374	-0.002591
3	-0.0365	-0.000250	0.2424	-0.000419
5	-0.00850	-0.000186	0.1349	-0.000765
10	-0.00259	-0.000060	0.0176	-0.000145

The values of **Table 5.2** were analyzed using **Minitab 18** to find out correlation among the co-efficients and the invasion radius. Using nonlinear regression method, it was found out that co-

efficient c and e follows asymptotic regression; whereas, co-efficient d and f follows power law which can be seen in **Figure 5.12**.

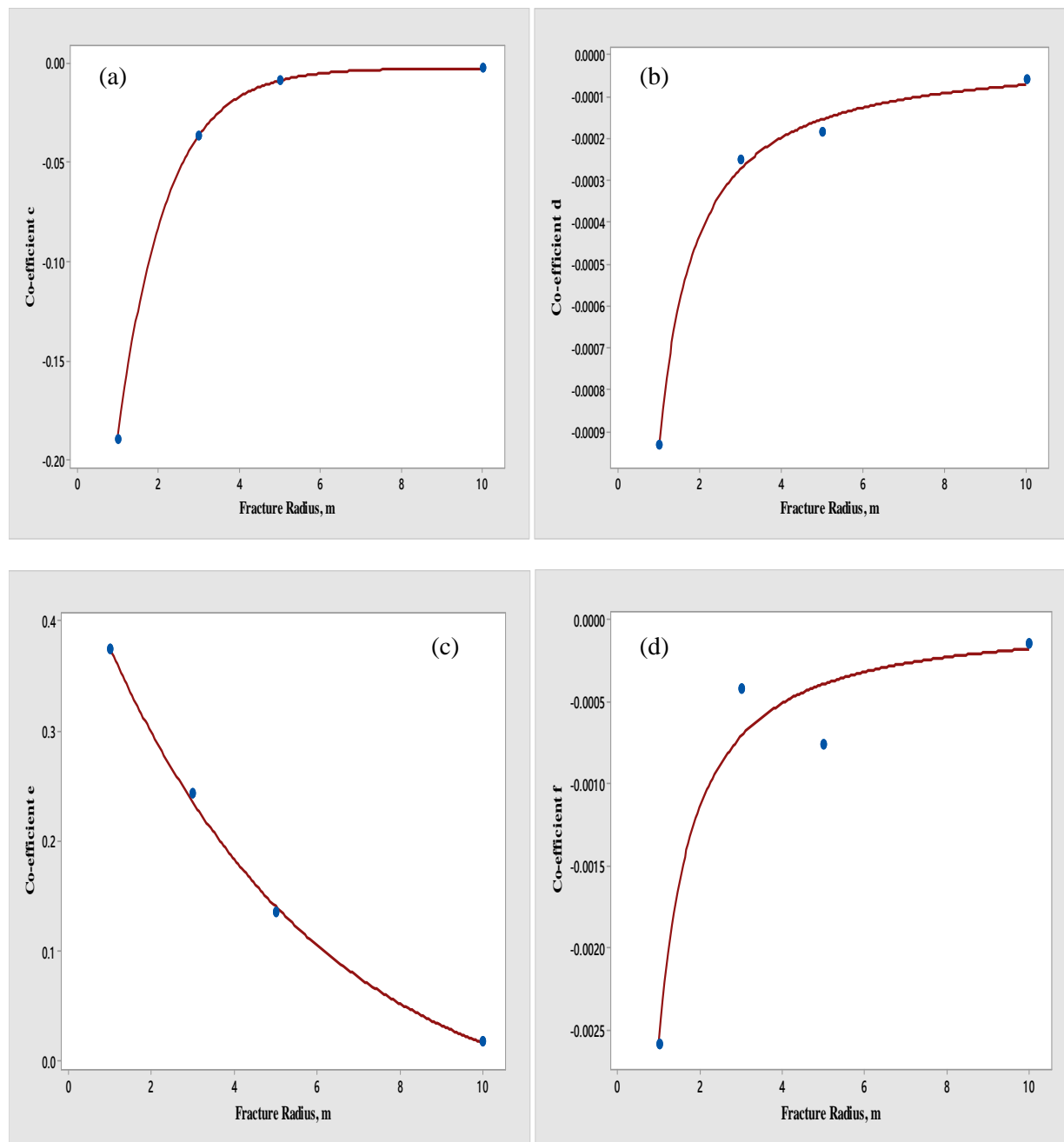**Figure 5.12: Effect of invasion radius on co-efficient c, d, e & f**

The trendline equations for **Figure 5.12 (a), 5.12 (b), 5.12 (c) and 5.12 (d)** are given by:

$c = -0.00242573 - 0.438962 * \exp(-0.852354 * R_i)$

$d = -0.000931342 * R_i^{-1.12184}$

$e = -0.0600066 + 0.529096 * \exp(-0.193715 * R_i)$

$f = -0.00256652 * R_i^{-1.17261}$

Replacing this equations of co-efficient c, d, e and f in **Equation 46 and 47**; and then replacing the equations of co-efficient a and b in equation 18 following correlation to determine drilling fluid velocity is found:

$$
\begin{aligned}
v = &\left[\{-0.00242573 - 0.438962 * \exp(-0.852354 * Ri)\} + \{-0.000931342 * R_i^{-1.12184}\}\right. \\
&\left. * \Delta P\right] \ln(Rh) \\
&+ \left[\{-0.0600066 + 0.529096 * \exp(-0.193715 * Ri)\}\right. \\
&\left. + \{-0.00256652 * R_i^{-1.17261}\} * \Delta P\right] \dots\dots\dots\dots\dots (48)
\end{aligned}
$$

Where,

v = Drilling fluid velocity inside rough fracture, ms^{-1}

ΔP= Overbalance pressure, psi

R_i= Invasion Radius, m

Rh= Roughness height, m

The velocity of drilling mud obtained from the equation is compared with the values obtained from the simulation and it was found that this correlation can predict the velocity of drilling mud inside a rough fracture with a tolerance of ±10%. However, this correlation is limited to the particular fluid properties stated in **Table 3.1**. Similar correlation can be constructed during onset of drilling by knowing the fluid properties, overbalance pressure and the roughness height.

Table 5.3: Comparison between the correlation and the velocity obtained from Fluent

Overbalance Pressure	Roughness Height, m	Invasion Radius, R_i	Fracture Velocity, v	Fluent Velocity (at 1m)	%Error
200	2.00E-05	1	3.909235	3.733687	-4.70172
200	4.00E-05	1	3.650231	3.498698	-4.33114
200	6.00E-05	1	3.498724	3.350413	-4.42665
200	8.00E-05	1	3.391228	3.246671	-4.45247
200	1.00E-04	1	3.307848	3.166805	-4.45379
500	2.00E-05	1	6.192412	6.579668	5.885647
500	4.00E-05	1	5.737941	6.087734	5.74586
500	6.00E-05	1	5.472093	5.80469	5.729797
500	8.00E-05	1	5.283471	5.599968	5.651771
500	1.00E-04	1	5.137164	5.438289	5.537132
800	2.00E-05	1	8.475589	8.58	1.21691
800	4.00E-05	1	7.825651	7.92522	1.25632
800	6.00E-05	1	7.445462	7.53273	1.15847
800	8.00E-05	1	7.175713	7.27534	1.36932
800	1.00E-04	1	6.96648	7.07897	1.58909
1000	2.00E-05	1	9.997708	9.76582	-2.3745
1000	4.00E-05	1	9.217458	8.95486	-2.9325
1000	6.00E-05	1	8.761041	8.50943	-2.9568
1000	8.00E-05	1	8.437208	8.20822	-2.7898
1000	1.00E-04	1	8.186024	7.98222	-2.5532

Table 5.3: Continued

Overbalance Pressure	Roughness Height, m	Invasion Radius, r	Fracture Velocity, v	Fluent Velocity (at 3m)	%Error
200	2.00E-05	3	1.055979	1.0251	-3.01215
200	4.00E-05	3	0.99491	0.97854	-1.67272
200	6.00E-05	3	0.959188	0.93421	-2.67364
200	8.00E-05	3	0.933842	0.91246	-2.34346
200	1.00E-04	3	0.914183	0.89552	-2.08412
500	2.00E-05	3	1.761719	1.905682	7.554384
500	4.00E-05	3	1.642274	1.795006	8.508695
500	6.00E-05	3	1.572404	1.723007	8.740733
500	8.00E-05	3	1.522829	1.673279	8.991305
500	1.00E-04	3	1.484377	1.631617	9.024197
800	2.00E-05	3	2.46746	2.55362	3.37394
800	4.00E-05	3	2.289638	2.39343	4.3366
800	6.00E-05	3	2.185619	2.2912	4.60797
800	8.00E-05	3	2.111816	2.21778	4.77787
800	1.00E-04	3	2.054571	2.16099	4.92448
1000	2.00E-05	3	2.937954	2.92542	-0.4283
1000	4.00E-05	3	2.721214	2.73316	0.43688
1000	6.00E-05	3	2.59443	2.61529	0.79751
1000	8.00E-05	3	2.504475	2.52747	0.9097
1000	1.00E-04	3	2.4347	2.46048	1.04785

Table 5.3: Continued

Overbalance Pressure	Roughness Height, m	Invasion Radius, r	Fracture Velocity, v	Fluent Velocity (at 5m)	%Error
200	2.00E-05	5	0.459041	0.50855	9.734577
200	4.00E-05	5	0.434166	0.48003	9.553758
200	6.00E-05	5	0.419615	0.46091	8.96005
200	8.00E-05	5	0.409291	0.44616	8.264179
200	1.00E-04	5	0.401284	0.43406	7.551994
500	2.00E-05	5	0.867233	0.96136	9.791141
500	4.00E-05	5	0.809076	0.89345	9.444121
500	6.00E-05	5	0.775057	0.84859	8.664856
500	8.00E-05	5	0.750919	0.80117	6.271714
500	1.00E-04	5	0.732197	0.7744	5.45029
800	2.00E-05	5	1.275424	1.29051	1.16883
800	4.00E-05	5	1.183986	1.19204	0.67534
800	6.00E-05	5	1.130498	1.1277	-0.2477
800	8.00E-05	5	1.092547	1.07684	-1.4586
800	1.00E-04	5	1.063111	1.02033	-4.1931
1000	2.00E-05	5	1.547552	1.47852	-4.6692
1000	4.00E-05	5	1.433926	1.3623	-5.2575
1000	6.00E-05	5	1.367458	1.28632	-6.3079
1000	8.00E-05	5	1.320299	1.22675	-7.6262
1000	1.00E-04	5	1.28372	1.15702	-10.951

Chapter Six: Future Work and Conclusion

Future Work:

Although this thesis has demonstrated the potential of simulation to determine fracture width and invasion radius from mud loss data, many opportunities to extend the scope of this thesis remain. A more accurate measurement of fracture width and invasion radius could be made by carrying out simulation incorporating following parameters:

- Variable overbalance pressure
- Variable fracture width
- Fluid leakoff through fracture walls

Conclusion:

It is of utmost importance to estimate the fracture width as soon as possible during lost circulation to facilitate a proper treatment procedure and to determine the particle size of the Lost Circulation Material (LCM) otherwise valuable mud will be lost and consequently, it will reduce the productivity of the reservoir by blocking the highly permeable fractures. By knowing rheological parameters from the mud report, during onset of drilling, correlations as shown in this study can be developed to determine invasion radius and fracture which will surely be useful to combat lost circulation and to design appropriate well development program more effectively. When lost circulation occurs, correlations developed during onset of drilling, it is possible to make an estimation of the fracture width which will indubitably be helpful in determining the particle size and the type of LCM to be used. Furthermore, in the well development stage, using the correlation of invasion radius, it is possible to determine the area that was damaged which will be very much useful to design a proper treatment scheme.

References

1) Feng, Y., Jones, J. F., and Gray, K. E.: "A Review on Fracture-Initiation and Propagation Pressures for Lost Circulation and Wellbore Strengthening" SPE 181747-PA, SPE Drilling & Completion, Vol. 17, Issue 2, pp. 131-144, May 2016

2) Wang, Y., Kang, Y., and You, L.: "Progresses in Mechanism Study and Control: Mud Losses to Fractured Reservoirs" Drilling Fluid & Completion Fluid, 24(4):74-77, 2007.

3) Cook, J., Growcock, F., Guo, Q.: "Stabilizing the Wellbore to Prevent Lost Circulation" Oilfield Rev. 23: 26–35, 2011

4) Mulder, G., Busch, V. P., Reid, I., Sleeswijk, V. T. J., and vanHeyst, B. G.: "Sole pit: Improving performance and increasing reserves by horizontal drilling." Proc., European Petroleum Conf., Society of Petroleum Engineers, Richardson, TX, 83–94, 1992

5) Gauthier, B. D. M., Franssen, R. C. W. M., and Drei, S.: "Fracture networks in Rotliegend gas reservoirs of the Dutch offshore: Implications for reservoir behavior, GeologieenMijnbouw/Netherlands." J. Geosci. (Prague), 79(1), 45–57, 2000

6) Nair, R., Abousleiman, Y., and Zaman, M.: "Modeling fully coupled oil-gas flow in a dual-porosity medium." Int. J. Geomech., 10.1061/ (ASCE) 1532-3641(2005)5:4(326), 326–338, 2005

7) Camac, B. A., Hunt, S. P., and Boult, P. J.: "Local rotations in borehole breakouts-observed and modeled stress field rotations and their implications for the petroleum industry." Int. J. Geomech., 10.1061/ (ASCE) 1532-3641(2006)6:6(399), 399–410, 2007

8) Li, Q., Wang, T., Xie, X., Shao, S., and Xia, Q.: "A fracture network model and open fracture analysis of a tight sandstone gas reservoir in Dongpu Depression, Bohaiwan Basin, eastern China." Geophys. Prospect, 57(2), 275–282, 2009

9) Dyke, C.G., Wu, B., and Tayler, D. M.: "Advances in Characterizing Natural-Fracture Permeability from Mud-Log Data" SPE 25022-PA, SPE Formation Evaluation, 1995

10) Sanfillippo, F., Brignoli, M., Santarelli, F. J., and Bezzola C.: "Characterization of Conductive Fractures while Drilling" Paper SPE 38177, SPE European Formation Damage Conference held in The Hague, Netherlands, 2-3 June 1997

11) Lietard, O., Unwin, T., Guillot, D., Hodder, M.: "Fracture Width LWD and Drilling Mud/LCM Selection Guidelines in Naturally Fractured Reservoirs", Paper SPE 36832 presented at the European Petroleum Conference, Milan, Italy, (Oct. 22-24), 181, 1996

12) Lie´tard, O., Unwin, T., Guillot, D. J., and Hodder, M. H.: "Fracture Width Logging While Drilling and Drilling Mud/Loss-Circulation-Material Selection Guidelines in Naturally Fractured Reservoirs" SPE Drilling & Completion, Vol. 14, No. 3, September 1999

13) Lavrov A. and Tronvoll J.: "Modeling Mud Loss in Fractured Formation" Paper SPE-88700-MS presented at the 11th Abu Dhabi International Petroleum Exhibition and Conference held in Abu Dhabi, U.A.E., 10-13 October 2004

14) Lavrov A.: "Radial Flow of Non-Newtonian Power-Law Fluid in a Rough-Walled Fracture: Effect of Fluid Rheology" Springer, Transport Porous Media 105:559–570, DOI: 10.1007/s11242-014-0384-6, 2014.

15) Majidi, R., Miska, S. Z., Thompson, L. G.:"Quantitative Analysis of Mud Losses in Naturally Fractured Reservoirs: The Effect of Rheology " SPE 114130, SPE Western Regional and Pacific Section AAPG Joint Meeting held in Bakersfield, California, U.S.A., 31 March- 2 April 2008

16) Bourgoyne Jr, A. T., Millheim, K. K., Chenevert, M. E. and Young Jr, F. S.: "Applied Drilling Engineering"; 2nd printing; SPE: Richardson, TX; pp 131-135, 1991

17) Razavi, O., Lee, H. P., Olson, J. E., and Schultz, R. A.: "Characterization of Naturally Fractured Reservoirs using Drilling Mud Loss Data: The Effect of Fluid Leak-Off" ARMA 17-855, 51st US Rock Mechanics / Geomechanics Symposium held in San Francisco, California, USA, 25-28 June 2017

Appendix A

ANSYS FLUENT provides the facility to attach user defined function (UDF) according to user's requirement. The UDF used in this study is written in C and defined using DEFINE macros. The function to calculate apparent viscosity is hooked through "Properties/Viscosity" at the "Create/Edit Materials" dialogue box.

The UDF code to calculate apparent viscosity is shown below:

```
#include "udf.h"

FILE *fp;

DEFINE_PROPERTY(hb_viscosity, c, t)

{

real viscosity;

real stress;

real ys;

real n, m;

real k;

real Max, Min;

n = 0.94;

ys = 4.022;

k = 0.04;

m = 1000;

Max = 100000;

Min = 0.00000000001;

stress = C_STRAIN_RATE_MAG(c,t);

viscosity = ys*(1-exp(-m*stress))/stress + k*pow(stress,n-1);

return viscosity;

}
```
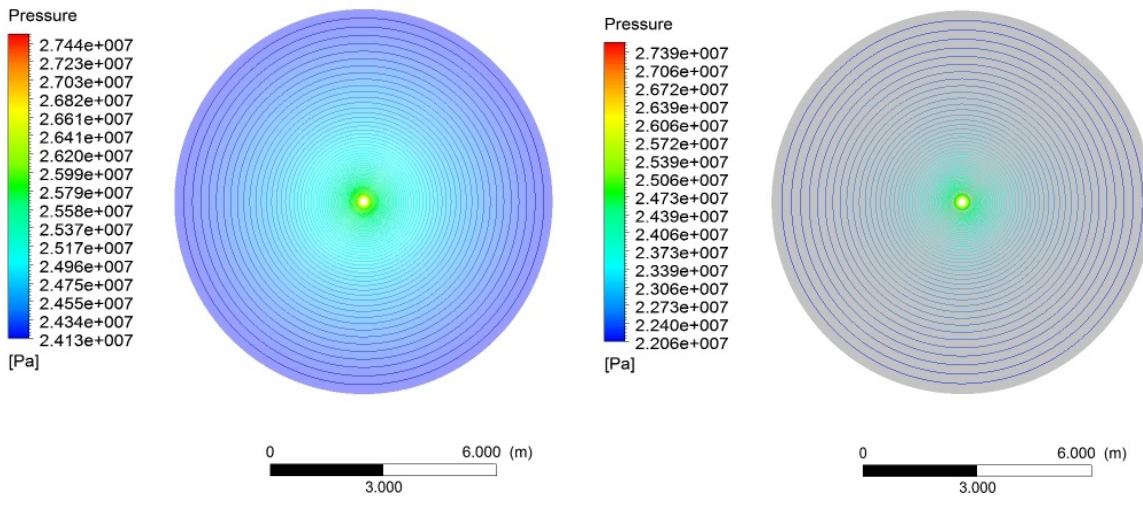
Appendix B

Figure B1: Pressure contour of smooth walled fracture: 500 Psi (Left) and 800 psi (Right)
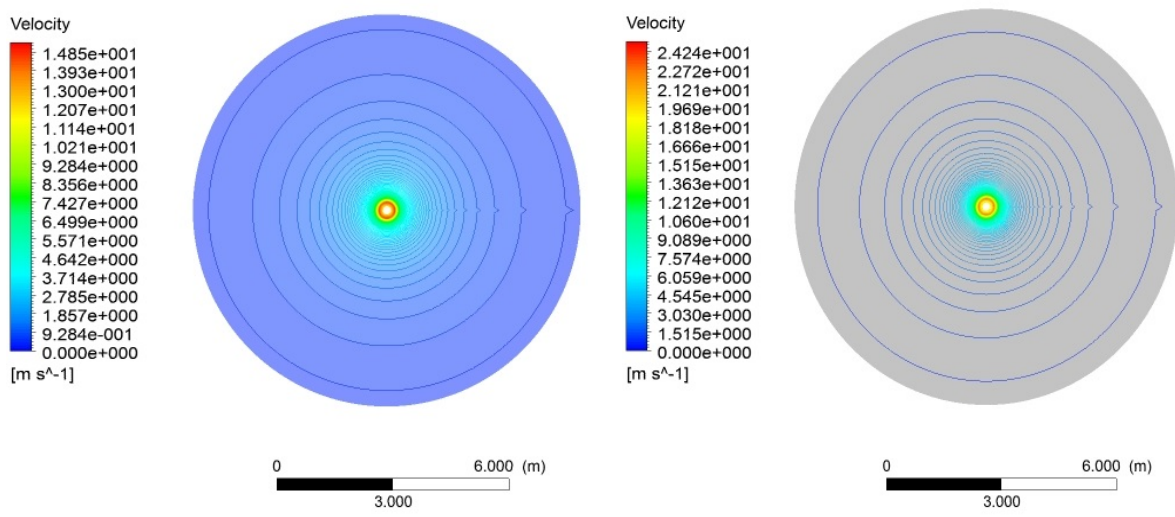

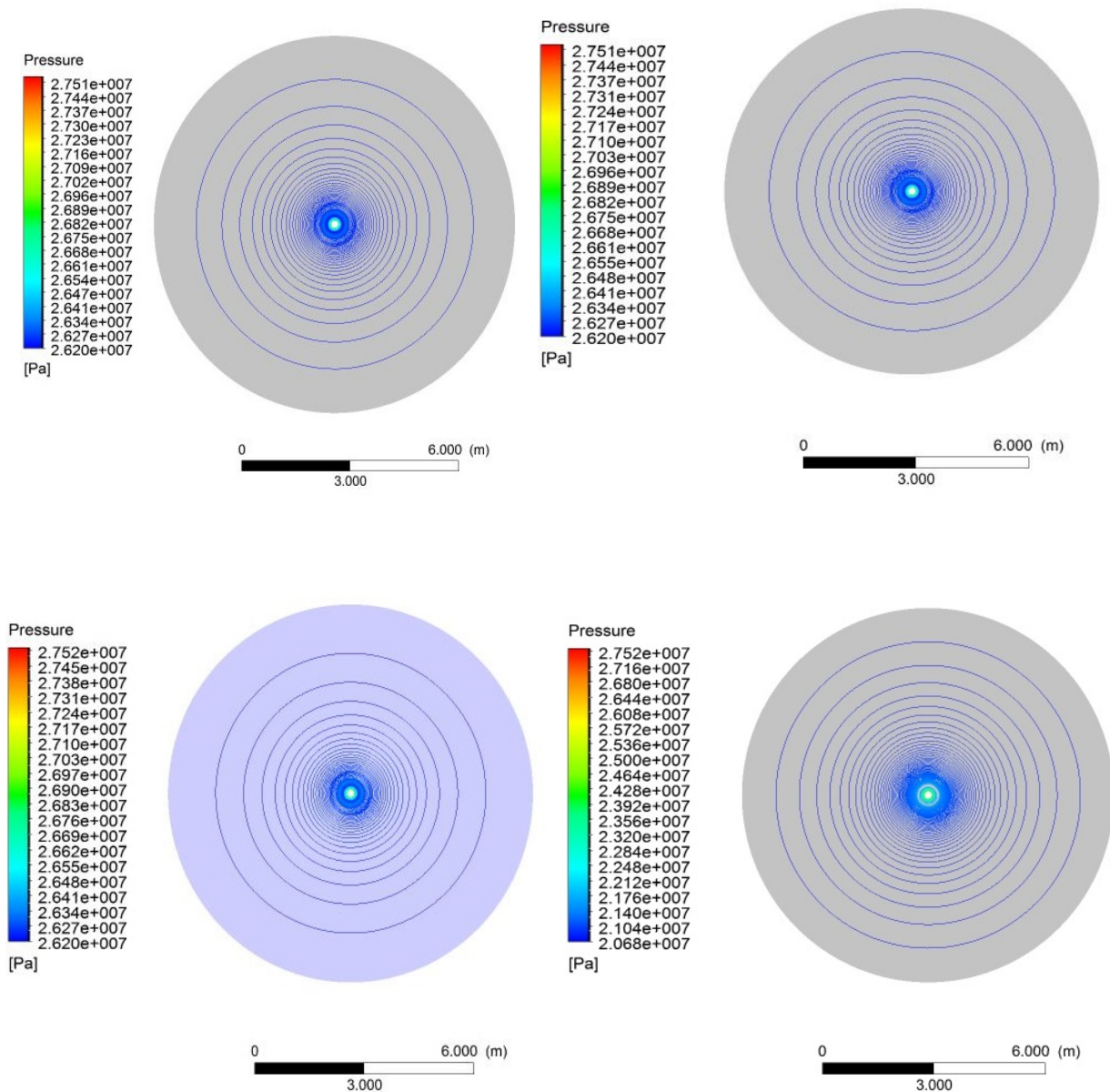**Figure B2: Velocity contour of smooth walled fracture: 500 Psi (Left) and 800 psi (Right)**

Figure B3: Pressure contour of rough walled fracture when Δp =200psi: Roughness height =4E-05 (Top left), Roughness height = 6E-05 (Top right), Roughness height=8E-05(Bottom left), Roughness height =1E-04 (Bottom right)

Figure B3: Velocity contour of rough walled fracture when Δp =200psi: Roughness height =4E-05 (Top left), Roughness height = 6E-05 (Top right), Roughness heigh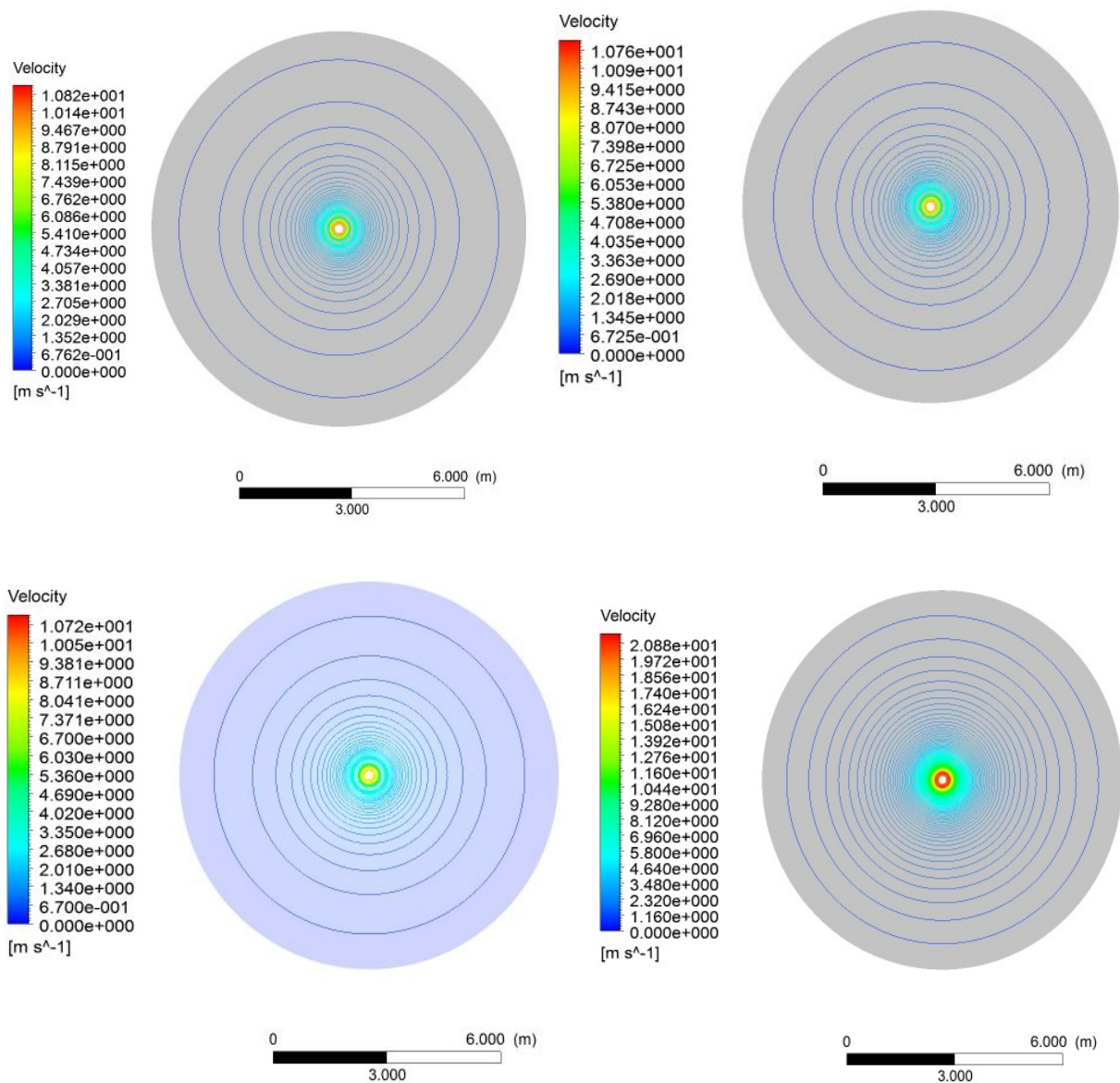t=8E-05(Bottom left), Roughness height =1E-04 (Bottom right)